Journal of Cardiovascular Magnetic Resonance®, 4(1), 129–162 (2002)

Poster Abstracts: Clinical MRI— Ischemic Heart Disease

265. T1 Weighted Myocardial Perfusion MR Imaging Using Blood Pool Contrast Medium SHU555C and Multi-Slice Hybrid Echo-Planar Sequence

Hajime Sakuma,[1] Kakuya Kitagawa,[1] Yasutaka Ichikawa,[1] Nanaka Ishida,[1] Kan Takeda,[1] Naoki Kato,[2] Satoshi Yoshise.[2]
[1]*Mie University, 2-174 Edobashi, Tsu, Mie, Japan;* [2]*Nihon Schering, 2-6-64 Nishimiyahara, Osaka, Japan*

Introduction: With recent advances in fast imaging techniques, contrast enhanced cardiac MR study can provide comprehensive assessments of myocardial perfusion, cardiac function and coronary anatomy in clinical patients. However, conventional gadolinium MR contrast agents demonstrate extracellular distribution, which makes it complicated to quantify myocardial perfusion because the contrast medium leaks rapidly from the blood pool to the interstitial tissue during first-pass. Ultrasmall superparamagnetic iron oxides (USPIO) agents have high T1 relaxivity and remain in the blood pool with a longer vascular half-life. These characteristics make USPIO agents potentially useful for assessments of myocardial perfusion, as well as for improving contrast on coronary MR angiography. However, the USPIO agent exhibits susceptibility effects as well, resulting in transverse dephasing and loss of signal which depend on a particle size of the USPIO agent and echo time of MR imaging sequence.

SHU555C is a small-molecular-size subfraction of frucarbotran (Resovist). The smaller size of the iron oxide particles in SHU-555C substantially reduces susceptibility effects and provides a larger $T1/T2^*$ relaxivity ratio. However, a feasibility of first-pass myocardial perfusion MR imaging using a bolus injection of the USPIO blood pool agent and a fast multi-slice perfusion MR sequence has not been demonstrated.

Purpose: In the current study, T1-weighted first pass myocardial perfusion MR images were acquired after bolus injection of SHU555C using a cardiac MR imager. The signal to noise ratio (SNR) and contrast to noise (CNR) were also assessed on 3D coronary MRA with navigator echo and fast cine MR images of the left ventricle before and after SHU555C administration.

Methods: MR studies were performed in six beagle dogs. The study protocol was approved by the institutional animal care and use committee. The animals were anesthetized and mechanically ventilated with a respirator. Each dog was placed supine on a plexiglas holder and inserted into a head coil in the magnet. MR images were acquired with a 1.5T cardiac MR imager (Signa CV/i, GE Medical Systems). After acquiring scout images, MR images were acquired as follows: (1) pre-contrast 3D coronary MR angiography, (2) pre-contrast breath-hold cine MR imaging, (3) first myocardial perfusion MR imaging, (4) second myocardial perfusion MR imaging after 15 minutes delay time, (5) post-contrast 3D coronary MR angiography, (6) post-contrast breath-hold cine MR imaging. Total MR imaging time excluding animal preparation was approximately 1 hour.

Myocardial perfusion MR images were obtained with a hybrid echo-planar sequence (TR/TE = 6.9/1.4ms, flip angle = 20 deg, ETL = 4, FOV = 32cm, Matrix = 128 × 128, slice thickness = 10mm). Interleaved notched saturation was used to optimize both T1 contrast (TI = 180ms) and number of slice locations. Seven short-axis images of the left ventricle were acquired every other heartbeats. Two sets of contrast enhanced perfusion MR images were acquired in order to assess feasibility of rest and stress perfusion MR assessments. In four animals, twenty micro-mol Fe/kg of SHU-555C was injected into antecubital vein as a compact bolus (<1ml) for each perfusion MR acquisition, followed by 10ml of saline flush at a rate of 3ml/sec with a power injector. In two animals, 0.1mmol/kg of Gd-DTPA was injected for comparison. Coronary MR angiography of the left main coronary artery and left anterior descending artery was acquired with a respiratory gated 3D MRA sequence using navigator echo (TR/TE = 5.6/1.5ms, flip angle = 30deg, FOV = 30 × 22.5cm, matrix = 256 × 160 × 14, slice thickness = 2mm). Breath-hold cine MR images were obtained on short axis and vertical long axis planes of the left ventricle, using a prospectively triggered fast gradient echo cine sequence with k-space segmentation (TR/TE = 6.7/2.3ms, flip

angle = 20 deg, views per segment = 8, FOV = 25cm, matrix = 256 × 128, slice thickness = 8mm).

Signal intensities on perfusion MR images were measured by placing regions of interest (ROI) in the LV cavity and myocardium. The SNR of coronary MR angiography was assessed by measuring signal intensity within the left main coronary artery (SNR = SI of blood / SD of noise). The CNR of cine MR images were measured at end-systole and end-diastole (CNR = [SI of blood − SI of myocardial]/SD of noise). Noise was measured as the SD of a ROI in an artifact free area of the images.

Results: Entry of SHU555C into the LV chamber caused a sharp increase in blood signal intensity, followed by an increase in myocardial signal intensity on both first and second sets of myocardial perfusion MR images. The peak signal intensities of LV chamber blood and myocardium after contrast normalized by pre-contrast myocardial signal intensity were 450% ± 20 and 166% ± 8 with SHU-555C, and 721% ± 26 and 217 ± 28 with 0.1mmol/kg of Gd–DTPA, respectively.

After administration of SHU555C, the signal intensity of the left main coronary artery on 3D coronary MRA increased to 319% ± 40 of the pre-contrast signal intensity. The averaged SNR of the left main coronary artery was 7.4 ± 1.8 before contrast and 28.9 ± 6.9 after contrast ($p < 0.01$).

The blood-myocardial contrast on fast cine MR imaging was also significantly improved after administration of SHU555C. The averaged CNRs of pre-contrast cine MR images on long axis plane were 11.7 ± 5.4 at end-diastole and 5.2 ± 1.7 at end-systole, which increased to 22.4 ± 4.4 and 18.8 ± 1.9 after administration of SHU555C ($p < 0.05$).

Conclusion: The results in this study showed a feasibility of T1 weighted first-pass myocardial perfusion MR imaging by using a bolus injection of USPIO blood pool agent SHU555C and a fast perfusion MR sequence. The administration of SHU555C can be highly useful for comprehensive cardiac MR study that evaluates myocardial perfusion, cardiac functions and anatomy of the coronary arteries.

266. Late Improvement of Regional Myocardial Wall Motion in the Area of Infarction After Acute PTCA in a 6-Month Follow-Up Using Delayed Contrast Enhanced Magnetic Resonance Imaging

Steffen Petersen,[1] Thomas Voigtländer,[2] Karl-Friedrich Kreitner,[1] Thomas Wittlinger,[3] Steffen Ziegler,[1] Georg Horstick,[1] Melanie Schmitt,[4] Wolfgang G. Schreiber,[1] Peter Kalden,[1] Oliver K. Mohrs,[1] Manfred Thelen,[1] Jürgen Meyer.[1]
[1]*University Hospital Mainz, Langenbeckstr. 1, Mainz, Germany;* [2]*University Mainz, Langenbeckstr. 1, Mainz, Germany;* [3]*University Hospital, Langenbeckstr.1, Mainz, Germany;* [4]*Johannes Gutenberg-Universitat Mainz, Department of Radiology, Mainz, Germany*

Introduction: Acute recanalisation in myocardial infarctions (MI) has been shown to be of benefit regarding the size of MI, the global myocardial function and prognosis (1–4).

Purpose: The aim of our follow-up study was to investigate the late effects of acute coronary angioplasty (PTCA) on regional wall motion after the subacute phase of MI. A significant improvement of global and regional wall motion is described after acute PTCA during the first week (5). Not much data exist on the long-term effects of acute PTCA on regional wall motion.

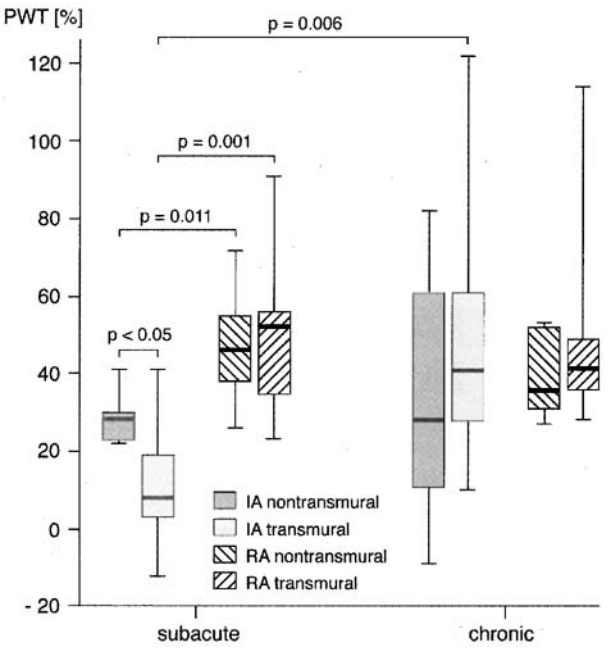

Figure 1.

Methods: 17 patients were investigated after acute PTCA in the subacute phase of MI and 6 months later at 1.5 T. Corresponding short axis slices encompassing the left ventricle (LV) were acquired for a standard cine MR and for delayed contrast enhanced magnetic resonance imgaging (ceMRI). Target parameters were the percentage size of infarction (PSI (%)) the percentage wall thickening (PWT (%)) in the infarct area (IA) and the remote area (RA) and global left ventricular function parameters (stroke volume index (SVI), end-diastolic (EDVI) and end-systolic volume index (ESVI)). Analysis was based on a 40 segment model.

Results: PSI was similar in the subacute phase and the follow-up (22.2 and 21.9 %, respectively; n.s.). Global left ventricular function did not change significantly over time. PWT improved significantly in IA (21.9 and 37.9 %, $p < 0.05$) in contrast to RA (46.4 and 38.4 %; n.s.). This late improvement could only be observed in transmural MI. There was a significant inverse correlation ($r = -0.54$; $p = 0.03$) between baseline PWT in the subacute phase of MI and the change of PWT over time.

Conclusion: PWT improved in IA after acute PTCA even after the subacute stage of MI in this 6-month follow-up study. PWT improved in transmural MI and in patients with a poor PWT in IA at baseline (11 days after MI). Delayed ceMRI as a tool to localise IA combined with regional wall motion analysis is a promising possibility to investigate long-term effects of reperfusion after acute MI.

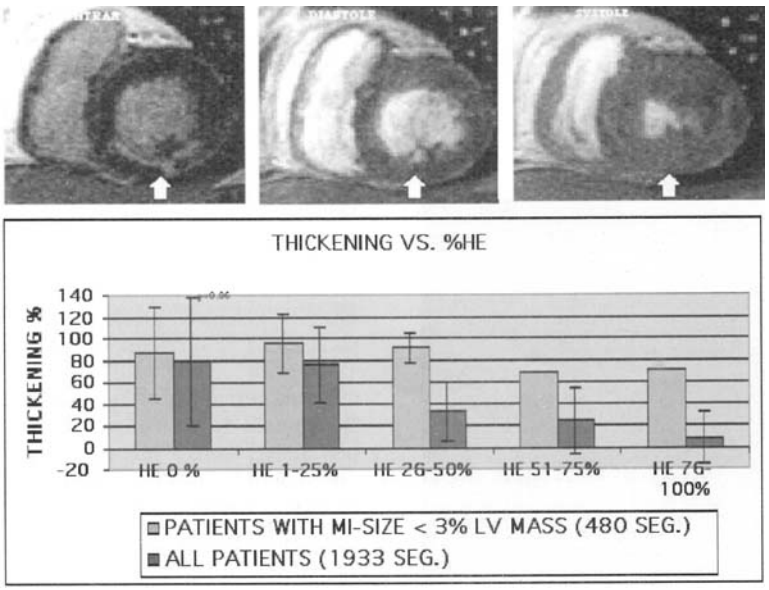

Figure 1.

267. Contrast MRI Detects Subendocardial Infarcts in Regions of Normal Wall Motion

Heiko Mahrholdt,[1] Anja Wagner,[1] Kelly Choi,[2] John Vargas,[1] Raymond Kim,[1] Robert Judd.[1] [1]*Duke Cardiovascular Magnetic Resonance Center, P.O. Box 3934, Durham, NC, USA;* [2]*Northwestern Medical School, 303 East Chicago Ave, Chicago, IL, USA*

Introduction: Patients with subendocardial myocardial infarction (MI) are at increased risk for future MI in the same territory.

Purpose: We hypothesized that after resolution of stunning wall motion by echocardiography, ventriculography, or cine MRI may be nearly normal despite the presence of subendocardial infaction.

Methods: We performed cine and contrast MR in 31 patients and 10 dogs. All patients had single vessel, first MI documented by enzymes, underwent successful reperfusion defined at catheterization, and were scanned at least 28 days later. Dogs underwent 90 min single vessel occlusion followed by reperfusion. Cine and contrast-enhanced MR (ce MRI) images were obtained. Wall thickening and transmural extent of hyperenhancement (HE) were measured quantitatively using a 72 segment model.

Results: For the 192 segments with less than 25% transmural MI extent, wall thickening was not different compared to the 1800 normal segments (figure and bar graph, above, dog $p = 0.86$, pts $p = 0.88$). In subjects with infarct size $< 3\%$ of total LV mass ($n = 11$) even transmural infarcted segments had normal wall motion if surrounded by normal moving neighbors.

Conclusion: Ce MRI can be used to identify clinically-important subendocardial infarcts in regions with normal wall motion.

268. TrueFISP Versus Contrast-Enhanced Magnetic Resonance Angiography for the Assessment of Coronary Artery Bypass Graft Patency

Nicholas Bunce,[1] Christine Lorenz,[2] Anna John,[1] Raad Mohiaddin,[1] Dudley Pennell.[3] [1]*Royal Brompton Hospital, Magnetic Resoncance Unit, London, England, UK;* [2]*Washington University in St. Louis, CMR Unit, London, United Kingdom;* [3]*Royal Brompton and Harefield NHS Trust, Sydney Street, London, United Kingdom*

Introduction: Assessment of coronary artery bypass graft (CABG) patency by cardiovascular magnetic resonance (CMR) has been performed with spin-echo and gradient-echo techniques with good sensitivity and specificity. However the diagnostic accuracy of these techniques has been affected by respiratory and motion artefacts, and total scan times can be excessive. Using ultra-fast gradient-echo sequences and a first-pass injection of gadolinium, it has become possible to obtain a 3D data set within a single breath-hold, and in small series the accuracy appears high. TrueFISP is a steady-state precession sequence that uses steady state imaging to produce white-blood images. Because of a low TE and TR, it is possible to perform a multi-slice or multi-phase image within a single breath-hold. Because of excellent contrast between blood and surrounding structures, TrueFISP sequences have been used to produce high-resolution images of the heart for use in ventricular function studies, without the need for a contrast agent. However this technique has not been used for the assessment of graft patency.

Purpose: We therefore investigated the diagnostic accuracy of multi-slice TrueFISP versus contrast-enhanced magnetic resonance angiography (MRA).

Methods: Twenty-five patients (mean age 63 years, range 39–84, all men) with previous bypass surgery, who had

Figure 1. TrueFISP

undergone recent diagnostic cardiac catheterisation for the investigation of angina, were studied with a Siemens Sonata 1.5T scanner. TrueFISP: Transverse and coronal breath-hold multi-slice images were acquired from the base of the heart to the subclavian vessels, using the following parameters, 8 slices, slice thickness 4 mm, voxel size 2.7 × 1.4 × 4 mm, TE 1.75 ms, TR 3.49 ms, flip angle 60°, temporal resolution 336 ms, ECG-gated to early-mid diastole. Breath-hold duration 8–12 seconds. MRA: A 3D coronal slab was positioned to include the heart and subclavian vessels. MRA was performed with a

Figure 2. MRA

Table 1.

Results from Cardiac Catheterisation

Diagnosis	Arterial Graft	Venous Graft	Total
Occluded	1	10	11
Patent	22	46	68

FLASH segmented-gradient-echo sequence with the following parameters, 32 slices per slab, slice thickness 2 mm, voxel size 1.6 × 1.6 × 2.0, TE 1.04 ms, TR 2.86 ms, flip angle 25°, temporal resolution 440 ms, ECG gated to early-mid diastole. Breath-hold duration 18–24 seconds. A pre-contrast study was performed, then a first-pass study was acquired during an injection of 0.2 mls/kg gadolinium–DTPA at a rate of 2mL/s. Analysis: CABG patency was determined from the cardiac catheter films. The CMR images were independently assessed by 2 observers, and a consensus diagnosis for graft occlusion obtained using a 3rd observer for any disagreements. TrueFISP images were assessed directly, but the MRAs were reviewed after MIP and MPR post-processing. Images were also qualitatively assessed using a visual score (0–4 with 0 poor and 4 excellent), and the time for analysis (including post-processing time) was measured.

Results: All patients completed the CMR with no complications. The results from cardiac catherisation are given in table 1. With CMR, the diagnostic results (for determining graft occlusion) are given in table 2. The mean visual score for TrueFISP was 2.9 and was reduced by flow artefacts particularly in patients with aortic valve disease. The mean visual score for MRA was 3.0 (p = n.s) and was reduced by respiratory artefacts. The mean time for TrueFISP analysis was 14.1 minutes versus 29.4 minutes ($p < 0.001$) for MRA including post-processing. A patent venous graft is shown with TrueFISP, figure 1, and MRA, figure 2.

Conclusion: Contrast-enhanced MRA with cardiac gating has a high specificity for graft patency and a moderate sensitivity for graft occlusion. Image quality is affected by respiratory artefacts due to the prolonged breath-holds, and mis-timing of the arterial gadolinium bolus. TrueFISP had a high specificity for graft patency but a low sensitivity for graft occlusion. Image quality is affected by flow artefacts. However the acquisition of multi-slice TrueFISP images, provides a rapid, non-invasive method for determining graft patency, and could be recommended for piloting prior to a contrast-enhanced MRA study.

Table 2.

The CMR Diagnostic Results

Technique	Sensitivity	Specificity	Accuracy
TrueFISP	45	84	78
MRA	73	85	84

269. Value of Intravenous Nitroglycerin Application to Improve Visualization of Coronary Arteries in Free Breathing Three-Dimensional Coronary MR Angiography

Matthias Hackenbroch,[1] Ulrich Hofer,[1] Carsten Meyer,[1] Sebastian Flacke,[1] H. Schild,[1] Torsten Sommer.[1]
[1]*University of Bonn, Sigmund Freud Strasse 25, Bonn, NRW, Germany*

Introduction: In vivo human and animal experiments have both shown that nitroglycerin usually causes dilatation of large epicardial capacitance coronary arteries and constriction of resistance vessels. Three dimensional bright blood coronary magnetic resonance angiography techniques have been successfully applied to visualize proximal and mid portions of the native coronary arteries in healthy and diseased states. In general, these gradient echo techniques are based on flow-related enhancement, resulting in bright blood visualization of the coronary arteries while signal of the surrounding myocardium and epicardial fat are purposefully attenuated.

It is not clear whether this nitroglycerin-induced dilatation of the large coronary arteries and the increase in coronary blood flow may improve the visualization of the coronary arteries during coronary MR angiography.

Purpose: The aim of this study was to evaluate if intravenously applied nitroglycerin improves 1. visualization of coronary arteries and 2. detection of coronary artery stenosis in coronary MR angiography.

Methods: 48 patients with suspected coronary artery disease underwent free breathing coronary MR angiography with real-time navigator correction (Intera, 1.5 T, Philips Medical Systems). An ECG-gated, fat-suppressed, 3D segmented-k-space gradient echo sequence (Turbo Field Echo, TR 7.4 ms, TE 2.2, 13 phase-encoding steps per cardiac cycle, in plane resolution 0.79 × 0.70) and a five-element cardiac phased array were used. Data acquisition was performed in mid-diastole. All patients underwent coronary angiography. Scans of the coronary arteries with and without intravenous nitroglycerin application (2.5 mg/h) to the patient were performed in random order.

Visualization of the coronary artery was qualitatively assessed using a four point grading scale (1: excellent, 2: good, 3: satisfactory, 4: poor).

The pathway of the coronary artery was reformatted and displayed in a single plane, from which the contiguous length and the diameter of the vessels were determined.

Equal segments of the left coronary artery (left main stem [LM], proximal LAD, proximal CX) and right coronary artery (proximal RCA, distal RCA) in the sequences with and without nitroglycerin were evaluated for 1. qualitative assessment of visualization of coronary artery, 2. measured vessel diameter, 3. measured vessel length and 4. detection of stenosis > 50% and compared with a 2-tailed paired Student's t test.

Results: The average lenght of contiguously visualized LM, LAD, CX and RCA was 2.2 ± 0.49 (SD) cm, 5.5 ± 1.9 cm, 4.6 ± 2.2 cm and 7.1 ± 2.4 cm in the scans without and 2.2 ± 0.37 cm, 5.6 ± 2.1 cm, 4.5 ± 2.0 cm and 7.3 ± 2.6 cm in the scans with application of nitroglycerin ($p > 0.05$).

The average diameter of LM, proximal LAD, proximal CX, proximal RCA and distal RCA was 6.8 ± 1.15 mm, 3.0 ± 0.48 mm, 2.9 ± 0.38 mm, 4.9 ± 0.70 mm, 3.3 ± 0.45 mm in the scans without and 6.9 ± 1.18 mm, 2.9 ± 0.47 mm, 2.9 ± 0.42 mm, 4.9 ± 0.73 mm, 3.3 ± 0.47 mm in the scans with application of nitroglycerin ($p > 0.05$).

The average score in the qualitative assessment of the visualization of LM, proximal LAD, proximal CX, proximal RCA and distal RCA was 2.0 ± 1.4, 2.2 ± 1.5, 2.4 ± 0.17, 2.0 ± 1.2, 2.6 mm ± 1.4 in the scans without and 2.0 ± 1.2, 2.3 ± 1.4, 2.4 ± 0.19, 1.9 mm ± 1.4, 2.5 mm ± 1.6 in the scans with nitroglycerin ($p > 0.05$).

There were no significant differences in the sensitivity [86% (24/28) vs. 82% (23/28); $p > 0.05$] and specificity [80% (16/20) vs. 85% (17/20); $p > 0.05$] in the detection of coronary artery stenosis between scans without and with nitroglycerin application.

Conclusion: Dilatation of proximal coronary arteries is the usual response to nitroglycerin observed during coronary angiography. The biochemical basis of the pharmacological action of organic nitrates is the release of nitric oxide from the nitrate group, which activates enzyme soluble guanylate cyclase, leading to the accumulation of cyclic guanosine monophosphate and subsequent vascular relaxation. Through this mechanism, organic nitrates exert a wide spectrum of physiological actions by dilating peripheral and regional arterial and venous smooth muscle coronary blood vessels, thus increasing coronary blood flow. Theoretically, these pharmacological effects have the potential to improve the visualization of coronary arteries using flow-related bright blood coronary MR angiography.

However, in patients with intravenously applied Nitroglycerin, we were not able to find any significant effects with respect to length of the contiguously visualized segment, vessel diameter, the acurracy and image quality in the detection of coronary artery stenosis.

The imaging quality of MR coronary angiography is mainly determined by the successful suppression of respiratory and cardiac motion. We hypothesize that the effects of Nitroglycerin on coronary arteries are too small to have a significant benefit on the visualization of the coronary arteries.

In summary we conclude that application of nitroglycerin does not improve the visualization of coronary arteries and detection of coronary artery stenosis in free breathing 3D bright blood coronary MR angiography.

270. MR Determination of Flow Reserve in Normal and Diseased Coronary Artery Bypass Grafts

Willemijn Bedaux,[1] Mark Hofman,[2] Stephan Vyt,[1] Jean Bronzwaer,[1] Cees Visser,[1] Albert Van Rossum.[3] [1]*VU University Medical center, De Boelelaan 1117, Amsterdam, Netherlands;* [2]*VU Medical Center, P.O. Box 7057, Amsterdam, Netherlands;* [3]*Free University Hospital, Department of Cardiology, MB Amsterdam, Netherlands*

Introduction: In patients after coronary artery bypass grafting (CABG), non-invasive testing may be helpful in the early detection of recurrent graft disease. Flow Reserve determined by Magnetic Resonance (MR) is a non-invasive test without use of ionizing radiation that has been demonstrated to identify significant coronary artery stenoses.

Purpose: The purpose of the study was to assess the value of MR determined graft flow reserve in differentiating non-obstructed from diseased saphenous vein grafts.

Methods: In 21 consecutive patients with a history of CABG and recurrent chest complaints, scheduled for X-ray coronary angiography, graft flow reserve was performed by MR. A 3D MR angiogram was obtained for the assessment of the course and the patency of the grafts. MR velocity encoded imaging was performed to quantify graft flow at baseline and during maximal hyperemia, obtained by intravenous administration of adenosine.

Results: MR was performed in 40 venous grafts (18 single and 22 sequential grafts), internal mammary grafts were excluded due to clip artifacts. In 3 grafts no flow measurements were performed because of MR angiographic occlusion confirmed by X-ray angiography. In 9 grafts a basal volume flow <20 ml/min was found, all demonstrating stenosis >50% by X-ray angiography. In remaining grafts (n = 28) flow reserve was assessed and divided in 3 groups; nonobstructed, stenoses > 50 %, and non-obstructed grafts with distal run-off to a stenosed native coronary artery or to a myocardial perfusion territory with old infarction classified as 'diseased graft run off'. A significant difference was found between graft flow reserve of grafts without significant stenosis with a normal run off (n = 10), and of grafts with stenosis < 50% or without significant stenosis but with diseased run off (n = 18) (2.5 ± 0.7 vs 1.8 ± 0.9, p = 0.04). An algorithm for detecting > 50 % stenosis combining basal volume flow < 20 ml/min and graft flow reserve < 2 had a sensitivity and specificity of 78 and 80 %, respectively.

Conclusion: Combined use of MR angiography and MR quantification of graft flow and flow reserve differentiates between normal and diseased venous grafts or graft run-off.

271. Direct Visualization of Infarcted Tissue by T1-Mapping in Patients with Acute Myocardial Infarction

Daniel Messroghli,[1] Thoralf Niendorf,[2] Jeanette Schulz-Menger,[3] Rainer Dietz,[4] Matthias Friedrich.[5] [1]*Franz-Volhard-Clinic, Humboldt University Berlin, Wiltbergstr. 50, Berlin, Germany;* [2]*GE Medical Systems, Milwaukee, Wisconsin, USA;* [3]*Franz-Volhard-Klinik, Wiltbergstrasse 50, Berlin, Germany;* [4]*Franz-Volhard-Klinik, Charite Campus Buch, Wiltbergstr. 50, Berlin, Germany;* [5]*Franz-Volhard-Klinik, Charite, Wiltbergstr. 50, Berlin, Germany*

Introduction: Acute myocardial infarction (AMI) leads to changes in myocardial relaxation properties. So far, infarct detection using Magnetic Resonance Imaging (MRI) techniques is mainly achieved by identifying delayed enhancement of contrast media.

Purpose: To examine whether quantitative T1-mapping could directly visualize changes of magnetic properties in AMI without the use of contrast media.

Methods: 8 patients with reperfused AMI (day 3 ± 1) underwent multi-breathhold MRI in a 1.5T system using a cardiac phased array coil. Images from calculated T1-values (T1-mapping) were generated. For each parametric T1 image, a set of 5 images with varying inversion times was acquired in a true short axis view prior to and after administration of contrast agent, using an inversion prepared fast gradient echo sequence (TE 1.0ms, slice thickness 15mm, mean acquisition time 16s per image).

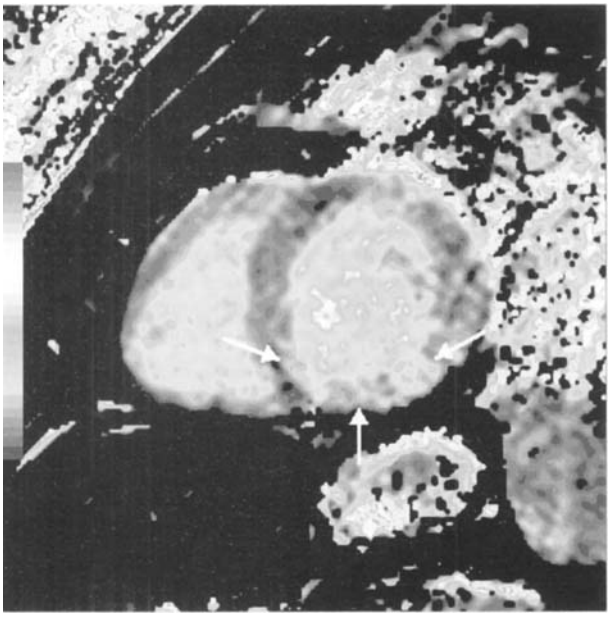

Figure 1. Pre-contrast T1-mapping, day 3 after inferior myocardial infarction.

Results: All patients showed a T1 prolongation in the area of infarction as identified by delayed enhancement, in agreement with the territory of the infarct-related vessel as detected by angiography. T1-values in the infarcted areas were found to be 118.1 ± 7.2% (SE) of those in remote areas ($p < 0.05$). The spatial extent of the area of T1-prolongation was larger than that of hyperenhanced areas in conventional contrast-enhanced images. After the administration of Gadolinium-DTPA (0.2 mmol/ kg), infarcted tissue showed a shortened T1-relaxation of 73.1 ± 3.8% as compared to remote areas ($p < 0.05$). The area correlated well to that of hyperenhancement in conventional contrast-enhanced images.

Conclusion: T1-mapping directly visualizes magnetic relaxation changes in acute myocardial infarction in patients. Post-contrast T1-maps reveal a shortened tissue relaxation of infarcted areas and correlate well to areas of increased signal intensity in contrast-enhanced images. In pre-contrast T1 maps, an area of prolonged T1-relaxation exceeds that of the necrosis as determined by contrast-enhanced imaging and thus may reflect transient pathophysiologic changes of adjacent tissue.

272. SPECT Versus MRI Measurements of Left Ventricular Volumes and Function over a Wide Range of Values

Sven Plein,[1] Penelope Thorley,[1] Timothy Bloomer,[1] John Ridgway,[2] Mohan Sivananthan,[1] [1]*Leeds General Infirmary, Gt. George Street, Leeds, West Yorkshire, United Kingdom;*

[2]*Leeds Teaching Hospitals, Department of Medical Physics, Leeds, West Yorkshire, United Kingdom*

Introduction: Gated Single Photon Emission Computed Tomography (SPECT) imaging is increasingly used in clinical practice to evaluate left ventricular (LV) volumes and function. Only a limited number of studies have compared SPECT measurements with MRI, which is the standard for measurements of LV volumes and ejection fraction and patient numbers in these studies have been small (1–3). Furthermore, new acquisition sequences, namely Steady State Free Precession (SSFP), have become widely used in MRI in recent years. Measurements of LV volumes with SSFP have been shown to differ from those with segmented k-space gradient echo (TGE) acquisition (4) and SSFP based measurements have not been compared with other imaging modalities such as SPECT.

Purpose: This study aimed to compare volumetric measurements between SPECT and MRI in a larger patient cohort with a wide range of LV dimensions, using both SSFP and TGE sequences for acquisition in MRI.

Methods: 50 patients (33 male, mean age 62 ± 8 years) who underwent SPECT scanning for clinical purposes were recruited for MRI study. 31 had a history of MI with abnormalities of wall motion on gated SPECT and 19 had normal wall motion. SPECT scans were performed on a Park Isocam II dual head gamma camera using 99m Tc Tetrofosmin. Gated data were acquired using 8 frames and were processed with quantitative SPECT software (Cedars-Sinai, Los Angeles, USA), which automatically calculates end-diastolic volume (EDV) and ejection fraction (EF). MRI scans were carried out on a Philips 1.5T INTERA CV system (Philips Medical Systems, Best, The Netherlands). Multi-phase data sets of the LV were acquired in short-axis orientation. In 17 patients a TGE sequence was used for image acquisition (TR 8.8 ms, TE 5.2 ms, flip angle 35°) and in 33 patients a SSFP sequence (TR 3.4, TE 1.7, Flip angle 55°). EDV and EV were measured manually using MASS software (Medis, Leiden, The Netherlands) by drawing endocardial contours in end-diastole and end-systole. Comparison was made between SPECT and MRI results using Bland-Altman and paired t-test and correlation coefficients were calculated. Data was analysed combined for TGE and SSFP and separately for the two MRI sequences. Comparison between TGE and SSFP used an unpaired t-test.

Results: SPECT estimations of EDV correlated with MRI measurements ($r = 0.90$), but were lower by a mean of 18.5ml (± 25.4), $p < 0.0001$ (see Table 1 and Figure 1). Similarly, there was a correlation for estimates of EF ($r = 0.84$) but SPECT measurements were lower by 6.54% (± 6.4), $p < 0.0001$ (Table 2 and Figure 1). Expressed as a relative difference, the mean results for SPECT were lower by a factor of 1.13 for both EDV and EF. Larger differences to SPECT were found for EDV with SSFP than with TGE (22.4ml vs 11.9ml, $p = 0.15$), while differences to SPECT in EF were similar for SSFP and TGE (5.9% vs 7.8%, $p = 0.33$).

Conclusion: We have found an overall agreement between SPECT and MRI measurements for EDV and EF in a wide range of patients. However there was a systematic difference between the two methods with MRI yielding larger values than SPECT. This may be partly due to differences in the definition of the endocardial border between the two techniques. The higher spatial resolution and better blood/myocardial contrast in MRI allow the identification of trabeculation, which is conventionally excluded from myocardial mass and included in

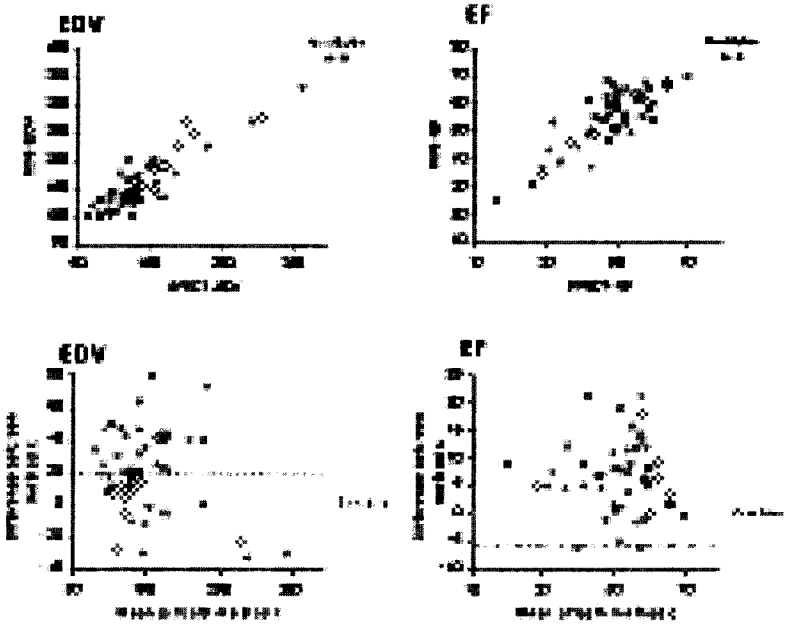

Figure 1.

Table 1

	Mean	SD	SE	r
SPECT-EDV	141.2ml	57.8	8.2	
MRI-EDV	159.6ml	51.6	7.3	
Difference	−18.4ml	25.4	3.6	0.90

Table 2

	Mean	SD	SE	r
SPECT-EF	48.5%	10.9	1.54	
MRI-EF	55.1%	10.6	1.49	
Difference	−6.6%	6.4	0.9	0.82

the volume. Due to the poorer resolution of SPECT, trabeculation cannot be separated from the endocardial border with this method, leading to lower volume estimates. SSFP acquisition in MRI further improves the delineation of the endocardial border, resulting in larger estimates of EDV and ESV (4). This was reflected in this study in larger differences for SSFP vs SPECT than TFE vs SPECT. The differences in EF between MRI and SPECT may also partly be a result of the lower frame rates in SPECT (SPECT 8 frames, MRI 12 frames for TGE, 18 frames for SSFP). A correction factor such as the factor of 1.13 calculated from our results, may be required for comparison of measurements of the two modalities.

273. Simultaneous Assessment of Wall Motion and Myocardial Perfusion During High-Dose Dobutamine Stress MRI Improves Diagnosis of Ischemia in Patients With Known Coronary Artery Disease

Andreas Wahl,[1] Stefan Roethemeyer,[1] Ingo Paetsch,[1] Sonja Huehns,[1] Eckart Fleck,[1] Eike Nagel.[1] [1]*German Heart Institute Berlin, Augustenburger Platz 1, Berlin, Germany*

Introduction: Recently, fast high-dose dobutamine–atropine stress MR (DSMR) has been shown feasible in patients with suspected or known coronary artery disease (CAD). DSMR has also been shown superior to dobutamine stress echocardiography (DSE) in patients with suspected CAD, a result attributed to superior image quality. However, as for DSE, around 10% of patients will have non-diagnostic submaximal negative test results because of an insufficient hemodynamic response to dobutamine–atropine administration or limiting side-effects. In addition, techniques based on assessment of regional left ventricular wall motion are in general more specific but less sensitive for detecting inducible ischemia, a finding in-line with the "ischemic cascade" theory stating that perfusion abnormalities precede wall motion abnormalities and ECG-changes. Since MR also enables the detection of myocardial ischemia using perfusion studies with high spatial resolution, with the unique possibility to quantitate myocardial perfusion with transmural resolution, and since high-dose intravenous dobutamine has been reported to fully exhaust myocardial resistance, like the direct coronary vasodilator adenosine, and regardless of the presence of mechanical dysfunction, a simultaneous assessment of wall motion and myocardial perfusion reserve during the same high-dose dobutamine–atropine stress test appears feasible.

Purpose: To determine whether a simultaneous assessment of wall motion and myocardial perfusion reserve during the same high-dose DSMR examination improves diagnosis of ischemia in patients with known CAD and prior coronary revascularization procedures. In this population, the diagnostic accuracy of noninvasive modalities is known to be limited.

Methods: 65 consecutive patients (mean age 59 ± 8 years; prior myocardial infarction: 63%; wall motion abnormality at rest: 83%) with revascularized CAD (prior PTCA: 90%; CABG: 28%) underwent DSMR (1.5 T; ACS NT, Philips, Best, The Netherlands) prior to clinically indicated invasive coronary angiography. DSMR images were acquired at rest and during a standardized high-dose dobutamine–atropine protocol during short breath-holds in 3 short-axis views (apical, midventricular and basal), a 4-chamber and a 2-chamber view. A single-slice turbo gradient echo technique (TE/TR/flip angle 5.6/1.9/20; spatial resolution $\leq 1.5 \times 2.5 \times 8$ mm; temporal resolution <25 ms) was used. All digital MR images were displayed as continuous synchronized cineloops using a multiple screen format (MASS software package, version 4.2, Medis, Leiden, The Netherlands) to compare corresponding rest, increasing stress and peak stress levels. Regional wall motion was assessed off-line by consensus between 2 blinded observers using a 16 segment model. Segmental wall motion was semi-quantitatively graded by a four-point scoring system (1: normal; 2: hypokinetic; 3: akinetic and 4:dyskinetic). DSMR was defined as positive for ischemia in the presence of a new or worsening wall motion abnormality in ≥1 segment. In the absence of ischemia, failure to attain 85% of age-predicted maximal heart rate was identified as a nondiagnostic result. During the same stress test (only at rest and at 20 ug.kg-1.min-1) 3 identical short axis views were acquired every heartbeat for perfusion measurements (inversion recovery single shot turbo gradient echo technique; pp-delay 200 ms; TE/TR/flip 3.6/12/30; spatial resolution $\leq 2.4 \times 2.4 \times 8$ mm). The upslope of the signal intensity time-curve of the first pass of a gadolinium–DTPA bolus (0.05 mmol/kg bodyweight) injected via an antecubital vein was determined at rest and during dobutamine infusion (MASS software package, version 4.2, Medis, Leiden, The Netherlands). Myocardial perfusion reserve was calculated from the alterations of the upslope. Segments were classified as ischemic or normal according to a previously determined threshold. For comparison with invasive coronary angiography, segmental wall motion and perfusion reserve were related to corresponding presumed coronary artery territories.

Results: Significant CAD (≥50% diameter stenoses by quantitative coronary angiography) was found in 65% of patients. In 6 patients (9%), wall motion analysis was non-diagnostic as target heart rate was not reached. The sensitivity and specificity of wall motion analysis for the detection of significant CAD were 85% and 74%, respectively. All patients with non-diagnostic wall motion analysis could be evaluated by

perfusion measurements, resulting in an overall sensitivity and specificity of 84% and 68%, respectively.

Conclusion: A simultaneous assessment of wall motion and of myocardial perfusion reserve during DSMR is feasible in patients with known CAD, and improves diagnostic yield compared to wall motion analysis alone.

274. Qualitative Regional Wall Motion Assessment Can Predict MRI or MUGA EF: An Objective Alternative to The Eyeball Ejection Fraction

Lilia Sierra-Galan,[1] Andrew Arai.[1] [1]*LCE/NHLBI/National Institutes of Health, Bldg 10, Room B1D416 10 Center Drive, Bethesda, Maryland, United States*

Introduction: While MRI provides a gold standard measurement of left ventricular (LV) volumes and ejection fraction (EF), quantitative analysis is time consuming and tedious. Automatic edge detection methods have improved substantially but still require clinical confirmation by a trained physician. Urgent clinical situations may require qualitative assessment prior to full quantification. For these and other reasons, physicians often rely on an "eyeball ejection fraction" as a method to estimate global LV function.

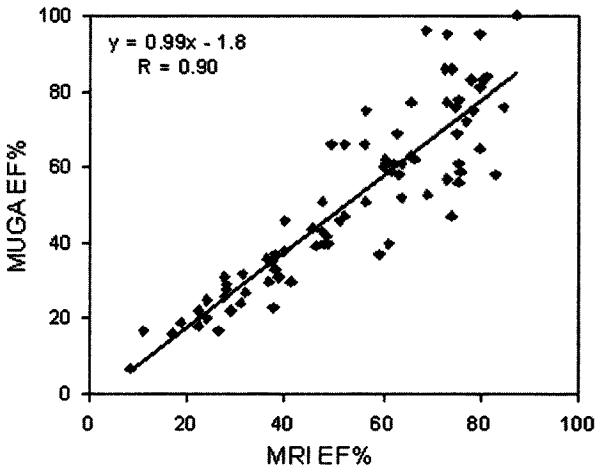

Figure 1. The conversion from ASE score index to MRI EF was based on the linear correlation in the initial 117 patients [y= − 21.863x+88.5, R=0.85]. The correlation improved by considering hyperkinetic segments based on a modified ASE score index incorporating 0 for hyperkinetic segments [y= − 20.552x+84.966, R=0.90]. Based on these correlations, LVEF was predicted on the independent cohort of 86 patients [fig 2: y=0.95x, R = 0.88]. Note, by failing to account for hyperkinetic segments, the predicted LVEF cannot exceed that associated with an ASE score index of 1.0. The correlation improved by considering hyperkinetic segments [y=0.99x, R=0.96].

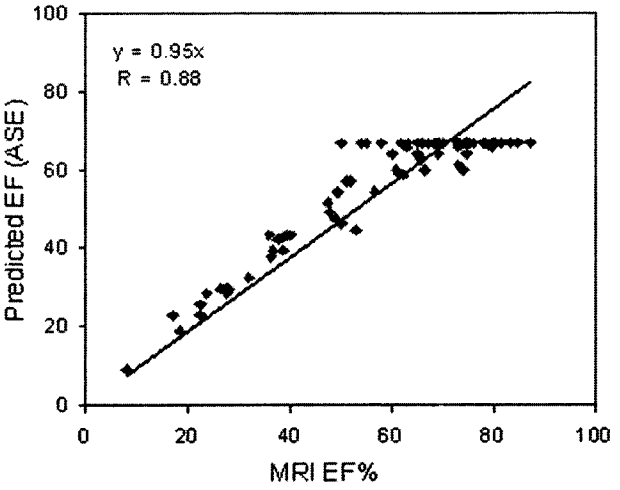

Figure 2. The ASE Predicted LVEF also correlated with MUGA EF [y=0.94x, R=0.68] and this correlation also improved by considering hyperkinetic segments [fig 3: y=1.00x, R=0.83].

We hypothesized that if the 16-segment model of the American Society of Echocardiography (ASE) accurately divides the myocardium in equal sized segments, the ASE Score index should correlate with global measures of contractile function such as LVEF. Since an accurate assessment of regional wall motion is an important part of the diagnostic summary of left ventricular function and is typically completed in a few minutes with no measurements, the ASE score index could provide an objective replacement to the widely used but difficult to describe "eyeball ejection fraction."

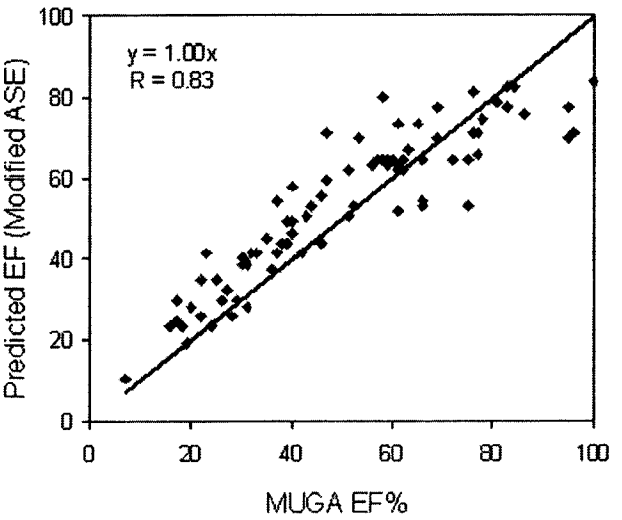

Figure 3.

Purpose: To create a mathematical model predicting LVEF by MRI from the ASE Score index of regional wall motion in a cohort of patients and then test the model in an independent group of MRI scans and also versus MUGA EF.

Methods: A group of 117 patients with a wide range of cardiac function was used to study the relationships between ASE score index and MRI LVEF. Another 86 patients were used as an independent group to confirm the validity of the model developed. In addition, 81 patients had radionuclide ventriculography (MUGA) available as a completely independent measurement of LVEF. MRI scans of LV function were quantified for LV volumes and EF by computer assisted planimetry. Regional wall motion was analyzed on cardiac MRI scans using the 16-segment ASE model (1 = normal, 2 = hypokinetic, 3 = akinetic, 4 = diskinetic, 5 = aneurysm). A modified ASE score index was calculated including a score index of 0 for hyperkinetic segments. Linear correlations in the independent cohort of 86 patients used y-intercept = 0 to minimize bias introduced by a few extreme values.

Results: All 3248 segments (100%) were analyzable for regional wall motion. MRI EF ranged from 8 to 87%. The MUGA EF correlated significantly with the MRI EF[fig 1: $y = 0.99x - 1.8$, $r = 0.90$].

Conclusion: An objective estimate of LVEF can be derived from qualitative regional wall motion analysis. The predicted LVEF correlates with MRI EF and MUGA EF as well as the two quantitative measures agree with each other. Since accurate assessment of regional wall motion is considered an important part of the diagnostic summary of cardiac studies like MRI and echocardiography, calculating this parameter from the ASE score index creates no additional burden on analysis or measurements. This method provides a systematic approach to deriving a qualitative assessment of LVEF which has been missing from common practices using an "eyeball EF."

275. Direct Myocardial Assessment of Systolic and Diastolic Heart Function Using HARP Analysis

G.M. Beache,[1] N.F. Osman,[2] A.Z. Faranesh,[2] D.A. Herzka,[2] M.T. O'malley,[3] C.A. Arnold,[2] J.L. Prince.[2] [1]*University of Maryland Medical Center, Dept. of Radiology, South Greene St., Baltimore, MD, USA;* [2]*Johns Hopkins University, N. Wolffe St., Baltimore, MD, USA;* [3]*University of Maryland School of Medicine, South Greene St., Baltimore, MD, USA*

Introduction: Regional contraction abnormalities are a hallmark of myocardial infarction (1), while impaired active relaxation is a sensitive indicator of abnormality in myocardial ischemia and in left ventricular hypertrophy (2).

Purpose: We used the harmonic phase (HARP) MRI technique for rapid quantification of tagged images, to explore the characterization of systolic and diastolic function in ischemic and in hypertrophic heart diseases.

Methods: Tagged, segmented gradient-echo images were acquired on a 1.5 T General Electric Signa (pulse sequence repetition time 4.1 ms; views-per-segment 16; tag separation 5 pixels; slice thickness 8 mm; flip-angle 12°; bandwidth ±64 kHz; field-of-view 28–32 cm; matrix 256 × 128) (Figure 1).

Resting studies were performed, in 3 healthy controls, a patient with a documented infarct with presumed regional systolic dysfunction, and 2 hypertension patients with documented mild and moderate left ventricular hypertrophy (HYP) with presumed graded reduction in global diastolic function. Rapid computation of left ventricular mid-wall regional circumferential strain from the tagged images was performed using HARP analysis (3). We generated contractile function curves using the mid-wall strain, plotted with respect to time within the cardiac cycle. To index regional systolic function we used the coefficient of variation (standard deviation/mean, among 4 myocardial segments) of the peak rate of shortening, computed using the time-derivative of the Fourier-fitted strain data. To index global diastolic function, we used the peak rate of early lengthening, which can be estimated visually as the relaxation peak slope, of the averaged regional strain plot.

Results: In the control subjects, peak rate of shortening had an average coefficient of variation of ~10 %. The infarct patient manifested decreased contraction coordination (coefficient of variation of ~20 %). As is apparent in Figure 2, the

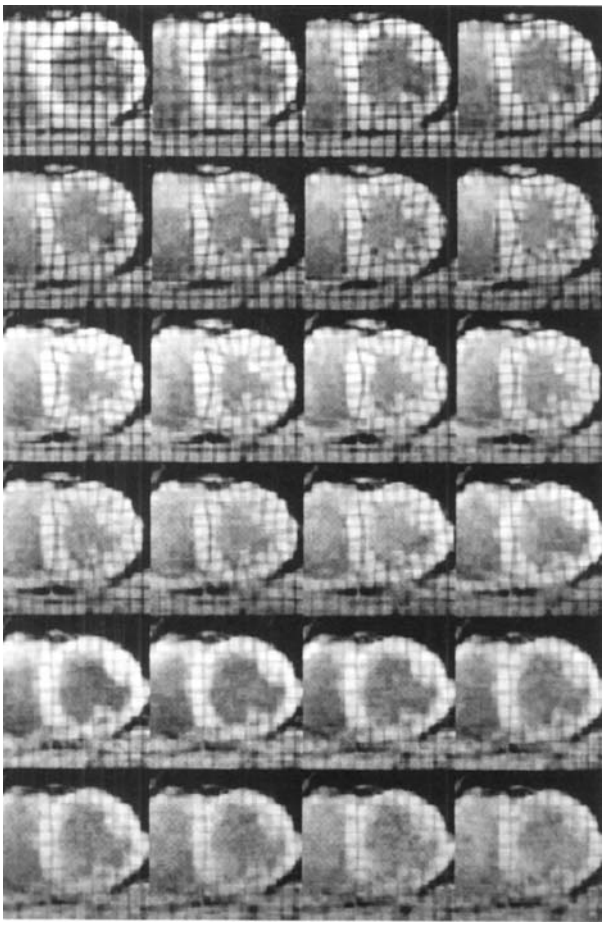

Figure 1.

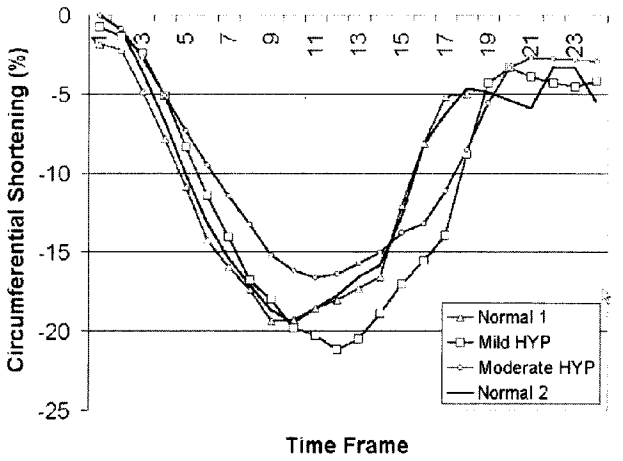

Figure 2.

relaxation peak slope was reduced in the patient with moderate hypertrophy, but not in the patient with mild hypertrophy.

Conclusion: Myocardial mechanics assessment by tagged MRI, with rapid HARP analysis has the potential to provide a sensitive means of indexing both regional systolic function (contraction coordination) and diastolic function (adequacy of active relaxation), and may yield new insights on the interaction between systolic and diastolic function.

276. Response of Diastolic Heart Function to Dobutamine Induced Stress

Bernard Paelinck,[1] Hildo Lamb,[2] Hugo Beyerbacht,[2] Anita Meiland,[2] Jeroen Bax,[2] Ernst Van Der Wall,[2] Albert De Roos.[2]
[1]*University Hospital Antwerp, Wilrijkstraat 10, Antwerp, Belgium;* [2]*Leiden University Medical Center, Albinusdreef 2, Leiden, The Netherlands*

Introduction: Stress-induced diastolic dysfunction is an early marker of myocardial ischaemia. The experience of MR dobutamine stress testing for systolic wall motion analysis is expanding. Studies of diastolic function during dobutamine stress however have been limited.

Purpose: To investigate the effect of dobutamine on left ventricular filling in healthy volunteers, assessed by MR flow mapping.

Methods: Mitral flow was measured in 10 healthy volunteers using a phase contrast fast-field echo (FFE) MR sequence. In all subjects, single-slice multi-phase echoplanar MR imaging was performed during free breathing with a Philips Gyroscan ACS-NT15. Imaging parameters included the following: echo-time = 4 ms, repetition time = 14 ms, flip angle = 20°, slice-thickness = 8 mm, field of view = 350× 280 mm, acquisition matrix = 128 and reconstruction matrix of 256. A velocity sensitivity of 150 cm/s was chosen. Two signals were acquired and a temporal resolution of 22 ms was achieved.

Results: Heart beat interval decreased from 841.8 ms ± 124.2 at rest to 543.0 ms ± 47.4 during dobutamine stress. The early (E) peak filling rate increased from 574.6 ml/s ± 103.8 to 718.2 ml/s ± 200.2 ($P < .05$) and the atrial (A) peak filling rate from 248.0 ml/s ± 64.0 to 369.0 ml/s ± 109.0 ($P < .001$) to yield an E/A peak flow of 2.4 ± 0.5 to 2.0 ± 0.3 ($P < .05$). E deceleration mean accelerated from $-3.2(ml/s2) \times 10 - 3 \pm 0.7$ to -4.3 $(ml/s2) \times 10 - 3 \pm 1.5$ ($P < .05$). E acceleration peak increased from 8.9 $(ml/s2) \times 10 - 3 \pm 1.7$ to 13.6 $(ml/s2) \times 10 - 3 \pm 4.6$ ($P < .05$). A deceleration peak accelerated from -4.2 $(ml/s2) \times 10 - 3 \pm 1.5$ to -8.5 $(ml/s2) \times 10 - 3 \pm 3.4$ ($P < .001$).

Conclusion: In healthy volunteers dobutamine stress enhances diastolic performance. This effect can be measured using a free breathing MR flow mapping sequence. These data provide a reference for further patient studies.

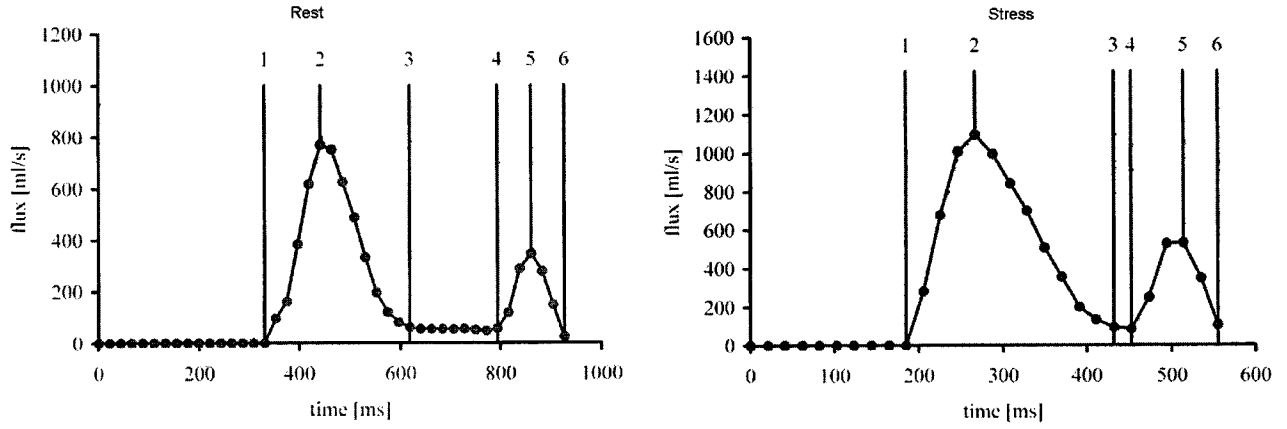

Figure 1.

277. A Comparison of Delayed Hyper-Enhancement to Resting First Pass Perfusion for Stress Perfusion MRI

James London,[1] Adam Schussheim,[1] Charles Marrota,[1] Christopher Konkus,[1] John Jacobacci,[1] Himanshu Verma,[1] Barry Cohen.[1] [1]*The Heart and Vascular Institute, 111 Madison Avenue, Morristown, NJ, USA*

Introduction: Cardiac MRI is emerging as a promising technique for stress testing. The ideal protocol to evaluate rest perfusion (RP) and stress perfusion (SP) has yet to be defined. Delayed hyper-enhancement (DH) imaging has been validated as an accurate method for the assessment of myocardial viability. DH may also provide insight into the assessment of resting myocardium in patients undergoing MRI stress testing.

Purpose: To compare DH to RP in patients undergoing MRI stress testing.

Methods: We performed both (DH) and (RP) on separate days in 75 patients (46 male, 29 female), age 60 ± 12 referred with a clinical indication for stress testing. Stress was achieved with dipyridamole (0.56mg/kg over 4 minutes). Patients were imaged on a 1.5 telsa scanner (Philips Intera CV, Nederland, B.V.). Six-slice (gating 2 × RR) first-pass perfusion imaging with gadolinium (0.1 mmol/kg) was performed using a fast gradient echo sequence with an echo-train readout. DH was performed using an inversion recovery sequence. Inversion time was optimized to null normal myocardium. Cine imaging was performed using a fast gradient echo sequence.

DH and RP were read qualitatively by one reader in a blinded fashion. The heart was divided using the 16-segment model. DH and RP were compared to determine concordance. Ejection fractions were calculated. Regional wall motion abnormalities (RWMA) were assessed qualitatively.

Results: SP abnormalities were seen in 24 patients (32%). 13 patients (17%) had either DH or RP abnormalities. DH and RP were concordant in 65 (87%) patients. In the 5 patients that DH was abnormal and RP was normal 4/5 had RWMA with ejection fraction (EF) 50% ± 14. In the five patients that RP was abnormal and DH was normal 0/5 ($p = 0.004$) had RWMA, EF 69% ± 9 ($p = 0.03$).

Conclusion: These findings suggest that DH is more accurate than RP at differentiating normal from nonviable myocardium. DH may provide important resting data for MRI stress testing.

278. Myocardial and Left Ventricular Function After Successful Primary Angioplasty of Anterior Wall Infarction Using MRI with Gadolinium-DTPA at Long Term Follow-Up

Knut-Haakon Stensaeth,[1] Pavel Hoffmann,[1] Nils-Einar Klow.[1] [1]*Ulleval University Hospital, Dept. of Cardiovascular Radiology, Kirkeveien 177, N-0407 Oslo, Norway*

Introduction: Primary angioplasty of acute myocardial infarction increase both short term and long term survival, and has been the preferred method of therapy of transmural myocardial infarction in our institution since 1996. It has been shown that left ventricular function is preserved in early stages using echocardiography and scintigraphic methods. MRI of the heart is a good examination to evaluate anatomical and functional parameters of the left ventricle. Recently, perfusion studies of the myocardium with MRI and contrast media have shown that MRI may also detect perfusion abnormalities of the myocardium. Knowledge is limited as to the long term findings of left ventricle (LV) function in patients with successful primary angioplasty (PCI) of acute myocardial infarction, whatever method being used.

Purpose: At long-term follow-up we aimed to examine the LV- and myocardial function with MRI and MRI-perfusion of patients with successful PCI of acute myocardial infarction, and include only patients with single vessel disease and successful PCI of the left anterior descending coronary artery (LAD).

Methods: From 1996 to 1998 one hundred patients were treated with PCI for acute transmural infarction. The angiography showed one-vessel disease in 55%, two-vessel in 25% and multivessel in 20%. The infarct related artery was LAD in 44%, the CX in 14%, the RCA in 41%, and bypass graft in one. 92% had TIMI 0 or 1 flow. Stent was placed in 73% and GPIIb/IIIa was used in 11%. Successful PCI was performed in 95%. Clinical follow-up was done in all 96 surviving patients. Sixteen patients met the criteria for MRI and consented to participate in the study. The study group comprised 13 men and 3 women, mean age at the time of the MRI was 59 ± 10 years. Follow-up was done after 19 ± 4 months after the primary PCI. All the patients had a clinical consult, exercise ECG and coronary angiography, and 13 patients had $^{99}Tc^{m}$-sestamibi gated single photon emission tomography (SPET). The MRI imaging procedure included a T1-weighted ECG-triggered multislice spin-echo sequence through the heart in the axial direction and 4 cine MR sequences of the LV. Cine MR was obtained by means of an ECG-triggered fast field echo-sequence and echo planar imaging (TE 8.8 ms, TR short, flip angle 30°), with slice thickness of 8 mm and a matrix of 256 × 256. The perfusion study was performed as a short-axis turbo field echo-sequence (TFE) in the mid LV plane. Contrast enhanced images were acquired with 0.05 mmol/kg Gadolinium-DTPA. T1-weighted inversion prepared TFE images were sequentially acquired, and a delayed set of 10–15 inversion recovery images was acquired in the same orientation 15 minutes after contrast administration.

Results: Only one patient had AP class 2, the others had minor symptoms from angina and dyspnoe. The ejection fraction (EF) at echocardiography had improved significantly in all but two patients, these patients also had increased hypoperfusion-index at SPET. During the follow-up period no patients experienced myocardial infarction, and no patients had any reintervention with surgery or PCI. Coronary angiography showed the LAD to be patent and without significant stenosis in 13 (81%). One was occluded, one was stenosed >90%, and one had reduced flow but no recurrent stenosis. One of these patients suffered from angina.

Mean values for the group were: end-diastolic volume (EDV) 135 ± 43 ml, EF 57 ± 16%, end-diastolic wall thickness (EDWT) of the anterior wall 12 ± 3 mm, and systolic wall thickening (SWT) of the anterior wall 54 ± 26%. EDWT and SWT were the same as the reference myocardium.

Four patients had EF less than 50%, from 28 to 44%, two of these with EF of 28 and 29%. Two of these patients had low SWT of the anterior wall, 12.5 and 14.3%. In one patient the LV myocardial wall thickness was globally reduced and the EDV increased to 235 ml. The intensity ratio between baseline and

the anterior wall at peak enhancement was 4.6 ± 2.2, at delayed images 2.5 ± 0.8, and the rate of signal increase over time (upslope) was 16.6 ± 12.5. These ratios were not different from the reference myocardium. The intensity ratio between the anterior wall and the inferior/lateral wall at peak enhancement was 1.3 ± 0.3 and the upslope was 1.5 ± 0.8. There was a tendency towards lower peak enhancement in those patients with reduced EF. The upslope also tended to be slower.

Conclusion: Clinically the patients had minor symptoms at follow-up. Our study indicates that successfull PCI of acute LV myocardial infarction preserved the myocardium in most patients at long term. However, in a few patients the LV myocardium did not recover. Overall there was no decreased enhancement of the anterior wall, although there was a tendency of decreased enhancement in patients with EF less than 50%.

279. The Impact of Myocardial Blood Flow and Gd Concentration on The Intravascular Component of Gd-DTPA During 1st-Pass Perfusion

Timothy Christian,[1] Anthony Aletras,[1] Robert Balaban,[1] Andrew Arai.[1] [1]*National Institutes of Health, NHLBI, LCE, Bethesda, MD, USA*

Introduction: MRI can image the first pass of gadolinium based contrast agents to evaluate myocardial perfusion at higher resolution than currently used nuclear perfusion methods. A first pass experiment simplifies interpretation of perfusion analysis with intravascular agents. Clinically approved gadolinium contrast agents rapidly enter the extracellular space and by definition exhibit more complicated kinetics.

Purpose: To determine the impact of increasing levels of myocardial blood flow (MBF) and concentrations of Gd-DTPA ([Gd]) on the myocardial time intensity curves (TIC) during 1st-pass Gd-DTPA perfusion.

Methods: Seven beagles were instrumented via open thoracotomy so that adenosine (20μgm/min/kg) could be selectively infused down a coronary artery. Gd-DTPA was infused in 6 dogs as a rapid bolus at 3 concentrations of Gd per dog: 0.025, 0.05 and 0.10 mmol/kg while running a saturation-prepared, segmented, echoplanar perfusion sequence. Imaging parameters included: 90° saturation pulse, T sat 10 ms, 15° readout flip angle, echotrain length of 4, field of view of 24 × 18 cm, and acquisition matrix of 128 × 72. This resulted in a temporal resolution of 147ms and a spatial resolution of 1.9mm × 2.5mm. A single dog had a true intravascular agent (0.05 mmol/Kg G7-DOTA) injected under the same conditions in order to map the intravascular TIC. Microspheres were injected directly after each infusion for MBF determination. TICs were created in remote and adenosine zones for each animal. Overshoot (OS) was defined from each TIC as the area between the TIC and the level of the recirculation curve (RC) so that it is normalized for any level of signal intensity as the RC forms the baseline of the measurement(see figure). The OS is an index of the intravascular component of the TIC while the remaining area under the TIC represents the interstitial component in the myocardium

Results: MBF values and OS area are shown in the table by dose and agent. MBF was not statistically different between the different doses of contrast agent. This was true both for the control zone and the adenosine region. MBF was significantly higher in the adenosine zone compared with the control region in all animals. Overall there was a significant difference in OS area between remote and adenosine zones for all 3 Gd concentrations studied. OS area did not differ by [Gd] for either the control or adenosine zones. By multivariate analysis, OS area was independently associated with MBF ($p < 0.0001$) but dose was not.

Conclusion: The most important finding of this study is that the TIC overshoot is highly dependent on blood flow but independnt of the dose of extracellular gadolinium contrast agent. This suggests that OS simply represented the vascular pool in the ROI and was not significant affected by transport limitations. These findings have important implications regarding the kinetics of the multicompartment models used to analyze myocardial enhancement in MRI first pass perfusion studies with extracellular Gd contrast agents.

TIC overshoot is a new index of the relative intravascular component of myocardial enhancement. We used this method as a semiquantitative tool that did not require assumptions about the fundamental kinetics we were interested in studying. While it is likely that more sophisticated analysis could further quantify the magnitude of these effects, the current method provides insight into the relative importance of MBF on the TIC. Most significantly, the intravascular to interstitial fraction shows minimal concentration dependence over a wide range of doses (0.025 mmol/kg to 0.1 mmol/kg).

Table 1

Results

	[Gd] 0.025	[Gd] 0.05	[Gd] 0.10	[G7] 0.05
MBF: control	0.57 ± 0.19	0.63 ± 0.23	0.67 ± 0.15	0.75
OS area: control	10 ± 28	2 ± 19	18 ± 45	214
MBF: adenosine	2.84 ± 1.18	1.80 ± 1.23	2.58 ± 1.41	2.14
OS: adenosine	87 ± 24	73 ± 17	87 ± 54	344

280. One and Two-Dimensional Algorithms Used for Estimation of Left Ventricular Mass Are Inaccurate in Patients with Distorted Left Ventricular Shape. A Comparative Study Using Magnetic Resonance Imaging.

Theano Papavasiliu,[1] Harald Kuehl,[1] Arnout Beek,[1] Albert Van Rossum.[1] [1]*VU University Medical Center, De Boelelaan 1117, Amsterdam, North Holland, The Netherlands*

Introduction: Assessment of left ventricular (LV) mass using 1-dimensional (D) and 2-D echocardiography is inaccurate in patients with distorted LV shape. These methods rely on mathematical models which require assumptions about LV geometry and image plane positioning, often not fulfilled using echocardiography. The value of the techniques for LV mass estimation with optimized position of imaging planes is not well established.

Purpose: In magnetic resonance imaging (MRI) data sets we determined LV mass assessed by 1-D and 2-D algorithms using optimized image plane position, and compared these to LV mass determined by the MRI slices summation method as reference standard in patients with distorted LV shape.

Methods: 22 patients (mean age 66 years) with LV aneurysms (ejection fraction 11–36%) underwent cardiac MRI on a 1.5T scanner (Magnetom Sonata, Siemens). Short-axis images covering the whole LV and perpendicular long-axis views were acquired using a True Fisp sequence (TE/TR 1.5/34ms, matrix 256 × 256, resolution 1.5 × 1.5 × 5mm). For the reference MRI end-diastolic endocardial and epicardial LV borders were traced manually in each short-axis image including papillary muscles. Calculation of LV mass using 1-D and 2-D algorithms was performed according to the recommendations of the American Society of Echocardiography (modified cube formula (MCF), area length (AL) and truncated ellipsoid (TEL) formula).

Results: Mean LV mass measured by MRI, MCF, AL and TEL was 17 ± 443g, 272 ± 71g, 205 ± 50g, and 197 ± 57g resp. ($p < 0.001$ for MCF vs. MRI and p = ns for AL and TEL vs. MRI). Correlations between MCF, AL as well as TEL and MRI were moderate ranging from $r = 0.48 - 0.69$. All algorithms overestimated MRI-LV mass (mean difference plusmn SD for MCF 99 ± 55g, AL 31 ± 47g and TEL 24 ± 41g; $p < 0.001$ vs. 0). The 95% confidence intervals for the differences between CMF, AL, TEL and MRI showed broad limits of agreement ranging from ± 82 to ± 110g.

Conclusion: Even with optimal image plane positions, LV mass assessed by 1-D and 2-D algorithms is inaccurate compared to the MRI reference standard. Thus, wrong geometrical assumptions account for the large differences in LV mass observed between the examined algorithms and MRI.

281. Global and Regional Mechanics Together with Reverse Remodeling After LV Reconstruction Surgery: A One Year 3-D MRI Analysis

Robert Biederman,[1] Mark Doyle,[2] Alistair Young,[3] Anton Fuisz,[4] Diane Vido,[1] Al Stanley,[5] Gerald Buckberg,[6] Constantine Athanaseulus,[5] Nathaniel Reichek,[7] Agostino Meduri,[8] David Mcgiffin,[2] James Kirkin,[2] Gerald Pohost.[2] [1]*Allegheny General Hospital, 320 East North Avenue, Pittsburgh, PA, USA;* [2]*University of Alabama at Birmingham, 320 East North Avenue, Birmingham, AL, USA;* [3]*University of Auckland, 320 East North Avenue, Auckland, New Zealand;* [4]*Washington Hospital System, 320 East North Avenue, Washington, DC, USA;* [5]*Carraway Hospital, 320 East North Avenue, Birmingham, AL, USA;* [6]*UCLA, 320 East North Avenue, Los Angeles, CA, USA;* [7]*St. Francis Hospital, 320 East North Avenue, Roslyn, NY, USA;* [8]*Istituto Di Radiologia Universita' Cattolica, 320 East North Avenue, Rome, Italy*

Introduction: Effects of surgical reconstruction on intramyocardial performance in end-stage dilated cardiomyopathy are poorly understood.

Purpose: To determine the relationship between altered LV volumetric indices and changes in regional intramyocardial function in patients undergoing surgical reconstruction therapy.

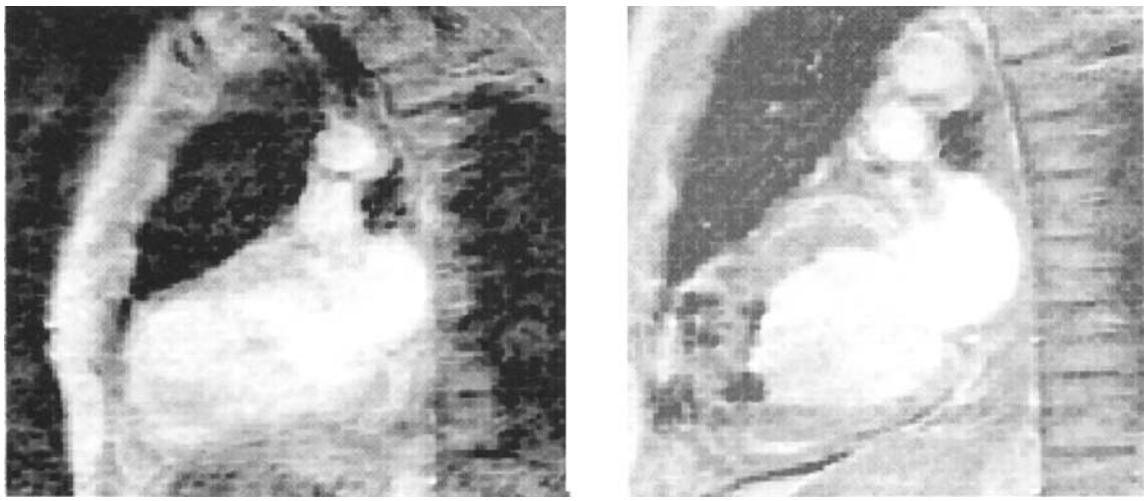

Figure 1. JW: PRE and POST Dor procedure.

Table 1

LV Remodeling Following LV Surgical Reconstruction

	LVEDV(ml)	LVESV(ml)	SV(ml)	EF(%)
Pre	296 ± 45	218 ± 36	78 ± 10	24 ± 4
Follow-up(12 ± 5mo)	210 ± 26*	143 ± 18*	90 ± 12*	32 ± 6*

*$p < 0.05$ vs. Pre

Methods: We studied 15 patients (59 ± 5 years—12M,3F) referred for the Dor procedure (LV endoventricular circular patch plasty) at 1 ± 1d prior (Pre), 2 ± 1mo (Post) and 1 year ± 5mo (Late). Two pts had MVR and all but one had CABG. End-diastolic volume, end-systolic volume, stroke volume, and ejection fraction (EDV, ESV, SV, and EF) were measured. A subset of six pts underwent 3-D MRI RF tissue tagging. Circumferential, radial, meriodonal, and circumferential–longitudinal (CL–shear) strains were measured using finite-element analysis. Principal minor and major strain were calculated from the strain tensor oriented in the circumferential direction. Specific investigation was directed towards the role of the reconstructed ventricular geometry. The LV was then divided into three regions: the *Repair* site, *Adjacent* and *Remote* myocardium.

Results: After the Dor procedure EDV and ESV decreased while SV and EF increased (see table and figure). Circumferential strain increased in the Remote but not the Adjacent or Repair regions by 19%: (7.3 ± 2.4 to 8.7 ± 2.3, $p < 0.05$ with no significant increase Late (8.9 ± 2.1). Meriodonal strain at the Repair site showed lengthening Post and a trend towards shortening Late with no significant changes in Adjacent or Remote regions. An increasing gradient in radial strain between Repair and Remote through Pre, Post and Late was present ($p < 0.05$). CL–shear was unchanged. Maximum principle strain increased at POST and remained so at FU (10 ± 4 to 15 ± 2 to 14 ± 5, ($p < 0.005$ for all). There was no significant difference in minimum principle strain. Phi, the angle between the circumferential direction and the minimum principle strain, changed PRE to LATE from −21 ± 16 to −10 ± 22°, ($p < 0.005$) becoming globally more circumferential. However, regionally, Phi become oriented more longitudinally and directly correlated with distance from the surgical patch (Repair).

Conclusion: Following LV reconstruction in patients with end-stage cardiomyopathy, reverse remodeling occurs which is coupled with improvements in intramyocardial mechanics predominantly in the remote myocardium at one year.

282. Can an Epicardial Nitinol Mesh Thwart Post-Infarct LV Remodeling?

Robert Biederman,[1] Leah Teekell-Taylor,[1] Sunil Mankad,[1] June Yamrozik,[1] Jane Ripple,[1] Walter Rogers,[1] Dennis Trumbull,[1] Kathleen Simpson,[1] James Magovern.[1] [1]*Allegheny General Hospital, 320 East North Avenue, Pittsburgh, PA, USA*

Introduction: Post-infarct remodeling inevitably ushers in a progressive downhill spiral whereby LV dilation begets further dilation culminating in intractable heart failure.

Purpose: We hypothesized that a device that could contain LV dilation after an infarct might retard this process. A Nitinol alloy mesh (Paracor) was specifically developed and investigated in a well-developed sheep infarct model.

Methods: Standard LAD occlusion by coronary ligation was performed in 14 sheep of which 7 were randomized to surgical implantation of a passive epicardial Nitinol mesh sutured to the AV groove that encompassed both the LV and RV. MRI (GE-CV/i) analysis of structure and function was performed prior to (Baseline) and 8 ± 1 weeks following (Post) infarct. The remaining 7 sheep served as a control arm. RF tissue tagging to characterize intramyocardial circumferential strain was performed on an available subset ($n = 11$; 5 mesh,6 controls) of the 14 sheep. Contiguous base to apex 7 mm slices were imaged and divided into 4 regions (septum, anterior, lateral and inferior) with a transmural (endocardial, midwall and epicardial) evaluation leading to 108 ± 12 strain measurements per heart. The analysis was further divided into *Infarct* (I), *Adjacent* (A) and *Remote* (R) zones and compared in a 2 × 2 fashion.

Results: Baseline characteristics were similar in each group. Placement of a Nitinol epicardial mesh resulted in blunting of the post-infarct remodeling process. LVEDVI, LVESVI and LV mass index were significantly reduced (see table). Importantly, LV mass index increased by 7% in control animals following infarction in contrast to a 13% decrease in the device group. No significant difference in mean circumferential segmental shortening (%S) was present at Baseline, nor was seen at Post (Adjacent 12 ± 6 vs 12 ± 7and Remote 15 ± 4 vs 15 ± 5 [$p = NS$ for all]). Despite this, significant regional differences were evident within each group and at each level pointing towards fundamental and unique differences in the mechanism of the remodeling process between the groups. For instance, in the control group there were no significant differences in %S in the Adjacent zone among the 4 regions measured, while in the mesh group there was a marked depression in %S in the inferior wall corresponding to the largest area of myocardium adjacent to Scar. Remarkably, %S was consistantly and significantly higher in the mesh group in *all* of the other regions as a function of both mean %S and transmural %S, ($p < 0.05$ for all). It therefore yielded no *net* change in *mean* %S in either group. No such regional heterogeneity was evident between groups on a regional basis in the Remote region. Finally, no histological

Table 1

Impact of Epicardial Nitinol Mesh on LV Remodeling

	LVEDV (ml/kg)	LVESV (ml/kg)	EF (%)	LVmass (g/kg)
Baseline mesh vs. control	1.9 ± 0.4 2.0 ± 0.7	0.9 ± 0.3 1.0 ± 0.5	54.5 ± 5.3 52.9 ± 8.2	1.9 ± 0.3 1.7 ± 0.1
Pos(8 ± 1wks) mesh vs. control	2.1 ± 0.3 2.8 ± 0.7*	1.3 ± 0.2 1.9 ± 0.6*	38.3 ± 5.5 33.7 ± 5.1	1.7 ± 0.4* 2.1 ± 0.4*

*$p < 0.05$ vs. Baseline

evidence of epicardial injury related to placement of the epicardial device was present on autopsy.

Conclusion: Nitinol epicardial mesh implantation significantly attenuates post-infarction LV remodeling and may favorably alter regional intramyocardial mechanics suggesting its clinical utility. A percutaneous model, currently under consideration, may allow deployment in human subjects in an acute setting.

283. MR Evaluation of Intracoronary Blood Flow and Correlation with the Aortic Flow in Patient with Coronary Artery Stenosis

Thomas Wittlinger,[1] Thomas Voigtländer,[1] Steffen Petersen,[1] Karl Friedrich Kreitner,[1] Jürgen Meyer.[1] [1]*2 nd Medical Clinic, University Hospital, Mainz, Rheinland-Pfalz, Germany*

Introduction: Significant coronary artery stenosis reduces the intracoronary blood flow at rest. The hemodynamic relevance is the most important factor for any interventionell procedures.

Purpose: It was the purpose of the study to evaluate the intracoronary blood flow at rest in patient with >70% coronary artery stenosis and to show a correlation to the aortic flow.

Methods: MRI flow measurements was performed in 20 patients (15 male, 5 female, age: 58.5 y) with >70% coronary artery stenosis. The flow determination (Magnetom Vision 1.5 T, Siemens AG) was done by using a Flash 2-D squence (TR 110 ms, TE 5 ms, VEC 250/75 cm/s) in breath-hold.

Flow was measured in the coronary artery (Venc 75 cm/s) and the aorta (Venc 250 cm/s).

In 10 healthy people flow measurements were done for controll.

Results: The mean coronary flow in correlation to the aortic flow was significantly ($p = 0.001$) reduced in patients with > 70% coronary artery stenosis. The LAD of the healthy subjects showed a predominantly diastolic flow pattern, the stenotic LAD a systolic flow pattern. There is no difference of the systolic or diastolic flow in the RCA

Conclusion: Velocity encoded MRI enables determination of flow in coronary arteries and in correlation to the aortic flow the detection of coronary artery stenoses.

Better results can be expected by flow measurements after pharmacologic stress testing.

Future developement should aim at the improvement of spatial and temporal resolution of the method.

284. Comparison of Vasodilator Myocardial Perfusion Using Cardiac MRI (cMRI) and SPECT Imaging

Maleah Grover-McKay,[1] Christopher Lisanti,[1] Jeffrey Dobkin,[2] Barbara Easterbrook,[3] John Messenger,[3] William Bradley.[1] [1]*Memorial MRI Center, 403 E Columbia St., Long Beach, California, United States;* [2]*Memrad, 100 Oceangate Ste 1000, Long Beach, California, United States;* [3]*Long Beach Memorial Medical Center, 2898 Linden Ave., Long Beach, California, United States*

Introduction: Like SPECT, cMRI can now perform multislice myocardial perfusion imaging. In addition, cMRI can evaluate cardiac anatomy and function and can detect myocardial infarction (MI) using delayed hyperenhancement (DHE).

Purpose: We hypothesized that results of vasodilator (VAS) myocardial perfusion imaging (VMPI) using cardiac cMRI and SPECT would be comparable for detection of normal, ischemic and infarcted myocardium, but cMRI would provide additional information regarding MI using DHE and other anatomic and physiological findings.

Methods: 11 patients (pts) in whom SPECT had been ordered for clinical indications underwent MRI and SPECT VMPI using the same VAS stress; the VAS was infused while the pt was in the MR imager (GE CVi). At maximal VAS effect, Tc-99m tetrofosmin was injected i.v. followed by Gd-DTPA.

Table 1

Results

	>70% Stenosis	>70% Stenosis	No CAD	No CAD
	Mean flow/RR	Flow%/Aorta	Mean flow/RR	Flow%/Aorta
LAD	0.286	0.66	0.82	1.54 p = 0.001
RCA	0.369	0.85	0.58	1.09 p = 0.001

First pass myocardial perfusion imaging (T1 weighted multi-shot EPI) imaging was performed immediately after VAS and 20 minutes later after injection of Gd-DTPA at rest. Subsequently, the pt underwent SPECT VMPI imaging and returned on another day for rest SPECT. MRI included long and short axis cine white blood images and, in 8 pts, DHE imaging to evaluate MI.

Results: cMRI and SPECT perfusion results were similar in 8 patients. In 1 pt, cMRI identified ischemia not described by SPECT and in another, the converse occurred. In 1 pt, cMRI identified a small fixed defect not described by SPECT. The DHE images confirmed known MI in 3 pts and identified 2 pts with small MI that were silent by history and ECG. Cine MRI diagnosed 2 pts with LVH, 1 with AI and 1 with pleural effusion.

Conclusion: cMRI and SPECT using the same VAS stress provided similar perfusion results. In patients with known or suspected coronary artery disease who are candidates for VAS VMPI, cMRI can identify 1) unsuspected MI using DHE imaging and 2) other anatomic and physiologic conditions, making it the preferred imaging technique.

285. Qualitative and Quantitative Analysis of Myocardial Perfusion Changes with Coronary Artery Angioplasty and Stent Implantation (PTCA) in Patients with Single Vessel Disease

Penelope Sensky,[1] Nilesh Samani,[1] Mark Horsfield,[2] Graham Cherryman.[2] [1]*Glenfield Hospital, Groby Road, Leicester, Leicestershire, United Kingdom;* [2]*Leicester Royal Infirmary, Infirmary Square, Leicester, Leicestershire, United Kingdom*

Introduction: Myocardial perfusion imaging with MR is now achievable on commercial imagers. MRI is ideal for serial perfusion imaging as no ionizing radiation is required for image acquisition. We have shown previously that both qualitative and quantitative image analysis are useful in the diagnosis of coronary artery (CA) disease (CAD) [1,2].

Purpose: To examine the use of both qualitative and quantitative image analysis in the serial evaluation of perfusion changes following CA revascularization with percutaneous angioplasty and elective stent implantation in patients with single vessel CAD.

Methods: Six consecutive patients (5 male, 1 female; mean age 57 ± 11 years) undergoing PTCA and stent implantation for single vessel CAD (>50% loss of angiographic cross-sectional area) were studied. CAD was present in the left anterior descending, circumflex and right coronary arteries in 3, 2 and 1 patients, respectively. All patients had grade 2 or 3 angina symptoms (New York Health Association criteria) and positive exercise electrocardiogram (ECG). Exclusion criteria were the presence of previous myocardial infarction, as defined by abnormal ECG or impaired systolic function on left ventriculography, and contra-indications to either MRI or adenosine infusion. First pass contrast MRI (1.5 Tesla MRI scanner, Siemens Vision, Germany) was performed within 7 days prior to PTCA (A), and then repeated within 7 days (B) of the procedure. A dynamic inversion recovery snapshot-FLASH sequence (TR = 4.5 ms, TI = 300 ms, TE = 2 ms, FOV 300 mm × 300 mm, slice thickness = 9 mm, 96 × 128 matrix, 25 measures) was used. Basal, mid-papillary and apical short axis planes were acquired after a bolus of 0.025 mmol/kg gadodiamide (Omniscan, Nycomed, UK) was injected at rest and during adenosine infusion (140 mcg/kg/min for 6 minutes). For image analysis, the myocardium was divided into 8 radial regions of interest (ROIs). These were assigned to the supplying CA territory according to the patient's individual angiographic CA anatomy as independently reported according to the Green Lane system [3,4]. An experienced radiologist, blinded to clinical and angiographic data performed qualitative image analysis. A perfusion deficit was defined as a ROI in which a reduced and/or delayed peak signal intensity following contrast enhancement was identified. Stress and rest images were reported together to allow recognition of normal perfusion, fixed (similar on rest and stress) and reversible (only apparent on stress) defects. The number of ROIs for each category was expressed as a fraction of the total number of ROIs supplied by remote and stenosed CAs, respectively. Quantitative analysis was independently performed on the mid-papillary slice of each examination. Epicardial and endocardial contours were traced by hand, and signal intensity and calculated relaxation rate time curves extracted for each ROI. The contrast bolus was similarly characterized from a ROI placed within the basal cavity to provide an input function. In combination with tissue data, the input function was entered into a deconvolution algorithm to calculate regional gadolinium unidirectional transfer coefficients (Ki) [5]. The stress/rest Ki ratios were calculated to give an index of myocardial perfusion reserve (MPRI) for each ROI [2]. A paired Student's t-test was used to evaluate haemodynamic and quantitative data. Perfusion at each visit in ROIs supplied by normal (remote) and stenotic / stented CA territories was compared.

Results: All patients completed the scan protocol. No adverse events or unexpected responses to adenosine occurred.

Table 1

Qualitative Image Data

	Visit	Normal	Reversible	Fixed
Remote	A	0.77(0.68 − 0.85)	0.23(0.15 − 0.32)	0(0 − 0.04)
Remote	B	0.85(0.76 − 0.91)	0.15(0.09 − 0.24)	0(0 − 0.04)
CAD	A	0.51(0.38 − 0.61)	0.47(0.34 − 0.61)	0.02(0 − 0.10)
stented	B	0.75(0.61 − 0.85)	0.24(0.14 − 0.37)	0.02(0 − 0.10)

Table 2

Quantitative Image Data

	Visit	Stress Ki	Rest Ki	MPRI
Remote	A	88.6 ± 44.9	42.3 ± 19.4	2.47 ± 1.75
Remote	B	110.3 ± 28.3	38.5 ± 19.8	2.94 ± 1.08
CAD	A	49.3 ± 23.5	49.2 ± 19.5	1.23 ± 1.06
Stented	B	93.3 ± 31.8	35.9 ± 13.2	2.78 ± 1.19

All patients improved symptomatically to NYHA class 0. Mean reporting time for qualitative analysis was 10 minutes per study (table 1; data expressed as confidence intervals for proportions). Mean time required to obtain quantitative data was 90 minutes per study (table 2; mean ± SD). No significant change in remote territory perfusion was detected with either reporting method. In territories originally supplied by stenosed arteries, following PTCA there was a significant increase in the number of normally perfused ROIs and reduction of ROIs demonstrating reversible perfusion deficits on qualitative analysis. Quantitative analysis demonstrated a significant rise in MPRI following revascularization ($p < 0.001$).

Conclusion: Qualitative and quantitative analytical methods are both of value in serial evaluation of myocardial perfusion following revascularization. Qualitative analysis is more appropriate in the clinical workplace because of the rapid reporting time. Until significant advances in analytical software occur, quantitative imaging is likely to remain a research tool.

286. Serial Assessment of Myocardial Perfusion Changes Following Transmyocardial Laser Revascularization (TMR) or Thoracic Sympathectomy (TS) in Patients with Refractory Angina

Penelope Sensky,[1] Manuel Galinanes,[1] Mahmoud Loubani,[1] Nilesh Samani,[1] Joseph Leverment,[1] Graham Cherryman.[1]
[1]*Glenfield Hospital, Groby Road, Leicester, Leicestershire, United Kingdom*

Introduction: TMR and TS are accepted therapeutic strategies in patients with severe coronary artery disease that is unsuitable for conventional surgical revascularization. It is unclear whether any clinical benefit is associated with changes in regional myocardial perfusion.

Purpose: To compare the effects of TMR and TS on regional myocardial perfusion.

Methods: Twenty consecutive patients (16 male, 4 female; mean age 65 ± 7 years) with intractable angina and coronary artery disease referred for surgical review were prospectively randomized to receive TMR or TS. Exclusion criteria were contra-indications to either MRI or adenosine infusion. First pass contrast MRI (1.5 Tesla MRI scanner, Siemens Vision, Germany) was performed within 7 days prior to the procedure (A), and then repeated 6 months (B) later. A dynamic inversion recovery snapshot-FLASH sequence (TR = 4.5 ms, TI = 300 ms, TE = 2 ms, FOV 300 mm × 300 mm, slice thickness = 9 mm, 96 × 128 matrix, 25 measures) was used. Basal, mid-papillary and apical short axis planes were acquired after a bolus of 0.025 mmol/kg gadodiamide (Omniscan, Nycomed, UK) was injected at rest and during adenosine infusion (140 mcg/kg/min for 6 minutes). For image analysis, the myocardium was divided into 4 equal radial regions of interest (ROIs) representing anterior, lateral, inferior and septal walls, respectively. Perfusion characteristics were compared in three groups: TMR treated ROIs (n = 27), non-lased ROIs and interventricular septum of the TMR patients (TMR control, n = 13) and ROIs in TS patients (n = 40). A perfusion deficit was defined as a ROI in which reduced and/or delayed peak signal intensity following contrast enhancement was identified. Stress and rest images were reported together to allow recognition of normal perfusion, fixed (similar on rest and stress) and reversible (only apparent on stress) defects. Transmural or subendocardial defect distribution was noted. The number of ROIs for each category was expressed as a fraction of the total number of ROIs in each group. Quantitative analysis was independently performed on the mid-papillary slice of each examination. Epicardial and endocardial contours were traced by hand, and signal intensity and calculated relaxation rate time curves extracted for each ROI. In combination with tissue data, the input function obtained from the basal cavity was entered into a deconvolution algorithm to calculate regional gadolinium unidirectional transfer coefficients (Ki) [1]. The stress/rest Ki ratios were calculated to give an index of myocardial perfusion reserve (MPRI) for each ROI [2].

Results: There was no change in angina (Canadian cardiovascular score) following TS (3.4 ± 0.5 vs. 2.6 ± 1.1, ns) but an improvement in symptoms was seen after TMR (3.6

Table 1

Qualitative Image Data

	TMR Lased		TMR Control		TS	
Visit	A	B	A	B	A	B
Normal	0.18 (0.11 – 0.27)	0.11 (0.06 – 0.19)	0.2 (0.09 – 0.37)	0.1 (0.04 – 0.26)	0.23 (0.16 – 0.32)	0.2 (0.13 – 0.29)
Reversible SE	0.32 (0.23 – 0.43)	0.38 (0.28 – 0.49)	0.23 (0.12 – 0.41)	0.4 (0.25 – 0.58)	0.46 (0.36 – 0.56)	0.19 (0.12 – 0.28)
Reversible TM	0.02 (0.01 – 0.08)	0 (0 – 0.04)	0.03 (0.01 – 0.17)	0 (0 – 0.04)	0.09 (0.05 – 0.17)	0.08 (0.04 – 0.16)
Fixed SE	0.21 (0.14 – 0.31)	0.19 (0.29 – 0.12)	0.27 (0.14 – 0.44)	0.17 (0.07 – 0.37)	0.16 (0.24 – 0.1)	0.3 (0.22 – 0.4)
Fixed TM	0.26 (0.18 – 0.36)	0.32 (0.23 – 0.43)	0.27 (0.14 – 0.44)	0.33 (0.19 – 0.51)	0.06 (0.03 – 0.13	0.23 (0.16 – 0.32)

Table 2

Quantitative Image Data

	Rest Ki		Stress Ki		MPRI	
Visit	A	B	A	B	A	B
TS	55.2 ± 35.2	40.9 ± 5.1	59.2 ± 32.9	54.6 ± 25.9	1.33 ± 0.99	1.55 ± 0.98
TMR lased	42 ± 17.1	46.6 ± 23.6	46.4 ± 17.9	50.2 ± 17.9	1.31 ± 0.74	1.2 ± 0.43
TMR control	41.6 ± 12.0	44.2 ± 29.1	58.5 ± 26.4	71.6 ± 38.4	1.48 ± 0.67	1.99 ± 1.27

± 0.5 vs. 1.9 ± 0.7, $p < 0.001$). However, no significant differences in perfusion characteristics as assessed by either qualitative (table 1; confidence intervals for proportions) or quantitative (table 2 mean ± SD) analytical methods were seen at rest or on stress between the three ROI groups or between preoperative and postoperative values within each group.

Conclusion: Despite an apparent clinical benefit following TMR, no change in myocardial perfusion was detected despite careful scrutiny of the subendocardium with qualitative analysis. Absence of improved perfusion with TMR and lack of clinical improvement with TS suggests that the perceived benefits of TMR are likely to be related to placebo effects rather than due to angiogenesis or cardiac denervation.

287. Improved TrueFISP Coronary Magnetic Resonance Angiography by Prolonging Breath-Holds with Preoxygenation

Richard Mc Carthy,[1] Steven Shea,[1] Vibhas Deshpande,[1] Jordin Green,[1] John Finn,[1] Debiao Li.[2] [1]*Northwestern University, 448 East Ontario Street, Chicago, Illinois, USA;* [2]*Northwestern University, Department of Radiology, Chicago, IL, United States*

Introduction: Elimination of respiratory motion in coronary magnetic resonance angiography (MRA) has generally been addressed in two separate ways. A navigator approach allows the subject to breathe freely during imaging and respiratory motion is compensated for by monitoring diaphragmatic motion. A breath-hold approach requires that image acquisition occur during suspended respiration.

TrueFISP (Fast Imaging with Steady-State Precession) has recently achieved widespread acceptance in cardiovascular imaging. It produces images with an inherently high signal-to-noise ratio (SNR). A recently developed technique for coronary MRA combines a breath-hold volume targeted approach and ECG-triggered, magnetizaton prepared, segmented 3D TrueFISP. The spatial resolution of images acquired with this technique is limited by breath hold duration.

Purpose: We instituted a study to examine the potential benefits of preoxygenation in 3D TrueFISP coronary MRA. We planned to investigate whether preoxygenation would prolong voluntary apnea during coronary MRA, and whether any increase in imaging time could be used to increase spatial

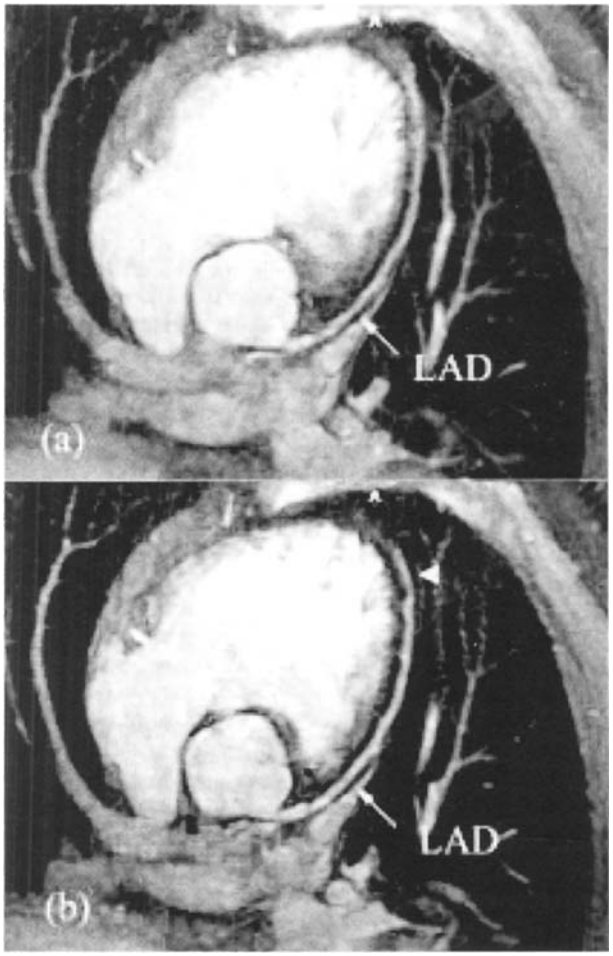

Figure 1. Paired room air (a) and post-oxygen (b) scans of the left main and left anterior descending (straight arrow) coronary arteries in a normal volunteer. (a) A room air image of the left main and left anterior descending coronary arteries (straight arrow) with a voxel size of 3.84 mm^3. (b) Post-oxygen image with a voxel size of 2.10 mm^3. Note the improved definition of the distal left anterior descending artery (arrowhead) on the higher resolution post-oxygen study.

resolution while maintaining acceptable image SNR. We also intended to evaluate the relative subjective comfort of room air and oxygen breath-holds.

Methods: Twelve healthy volunteers completed the study satisfactorily. The maximum comortable duration of voluntary apnea with and without preoxygenation was determined for each subject. Each subject then underwent coronary MRA with and without preoxygenation. The parameters for each coronary MRA study were adjusted to take advantage of the maximum time available for imaging. Subjects were asked to grade the relative difficulty of the oxygen and room air breath-holds.

The MR examinations were performed on a 1.5 T whole body scanner (Magnetom Sonata,Siemens Medical Systems, Erlangen, Germany) with a high performance gradient subsystem (maximum gradient strength: 40mT/m, maxmum gradient slew rate: 200mT/m/sec)

The images obtained from room air and oxygen breath-holds were compared by calculating the voxel size and SNR for each imaged vessel.

Results: The median improvement in breath-hold duration following preoxygenation was 38.5 seconds (12.0–68.0 seconds). This difference was found to be statistically significant ($p \ll 0.001$). The average voxel size decreased from $3.28 \pm 1.08\,mm^3$ on the room air scans to $1.80 \pm 0.67\,mm^3$ on the post-oxygen scans ($p \ll 0.001$). The average SNR decreased from 15.85 ± 8.07 on the room air scans to 11.75 ± 5.04 on the post-oxygen scans ($p = 0.002$). Oxygen breath-holds were rated as significantly easier than those on room air using the Wilcoxon signed rank test ($p = 0.0053$).

Conclusion: This study has shown that preoxygenation is a practical and well-tolerated technique in healthy volunteers undergoing coronary MRA and can produce images with increased spatial resolution as well as enhanced subject comfort. Clearly these results need to be repeated in a patient population for the technique to be useful clinically. However, we feel that this is a promising technique, which may prove useful in improving the diagnostic accuracy of coronary MRA.

288. Magnetic Resonance Imaging Evaluation of Double Blind Percutaneous Myocardial Revascularization with The Holmium YAG Laser

Pavel Hoffmann,[1] Knut-Haakon Stensaeth,[1] Kjell Inge Gjesdal,[1] Nils-Einar Klow,[1] Sindre Stavnes,[1] Magne Brekke.[1]
[1] *Ullevål Hospital, Dept. of cardiovascular radiology, Oslo, Norway*

Introduction: Myocardial laser revascularization is an experimental treatment for patients with angina pectoris (AP) that is not suitable for angioplasty (PTCA) or for coronary artery bypass grafting (CABG) and which also is refractory to medical therapy. Although results of clinical studies suggest that this treatment is efficient in relieving angina, the technique remains controversial and little is known about how the laser percutaneous myocardial revascularization (PMR) improves the patients' AP. Both angioneogenesis, resulting in improved blood supply to the ischemic myocardium, and increased scar

Table 1

LV EF at Control Angiography and MRI LV EF and LV EDV Prior to, First Day After and at 3 Months Follow up After Laser PMR Treatment

	Laser			Sham		
	Pre	Day 1	3 Months	Pre	Day 1	3 Months
LV EF (angiography, %)	66 ± 17			71 ± 16		
LV EF (MRI, %)	64 ± 12.	68 ± 17	68 ± 9	71 ± 19	74 ± 15	76 ± 11
LV EDV (ml)	126 ± 46	133 ± 36	125 ± 46	134 ± 30	137 ± 35	139 ± 35

All values are presented as mean ± SD. No significant changes.

Table 2

Signal Intensity (SI) in the Laser PMR Treated Region of the Left Ventricle. Control, Maximal SI and Delayed Day After Enhancement Prior to, First and at 3 Months Follow up After Laser PMR Treatment

	Laser			Sham		
	Pre	Day 1	3 Months	Pre	Day 1	3 Months
Control (SI, %)	100	100	100	100	100	100
Maximal enhancement (SI, %)	761 ± 562	708 ± 431	933 ± 561	998 ± 589	878 ± 526	1078 ± 545
Delayed enhancement (SI, %)	232 ± 176	215 ± 120	272 ± 182	346 ± 194	389 ± 209	340 ± 212

Values are presented as % of control ± SD. No significant changes.

tissue formation, resulting in decreased oxygen demand have been suggested. Also other mechanisms, like denervation have been discussed.

Purpose: The purpose of the present study was a MRI evaluation of myocardial function, measured as wall thickening and ejection fraction (EF) in patients undergoing laser PMR. To study whether there may be an angioneogenesis following PMR, myocardial perfusion was performed. Scar tissue formation was validated by the delayed hyper enhancement method.

Methods: The present MRI study was performed in a subset of 24 patients included in the Blinded Evaluation of Laser (PMR) Intervention Electively For angina pectoris "BELIEF" study by Nordrehaug and co workers (ACC 2001). The PMR study was randomised and double blinded including patients in NYHA class III and IV angina pectoris with reversible ischemia, not suitable for CABG or PTCA. The PMR procedure was performed with Holmium YAG laser or as a complete sham intervention with a non-active catheter. 12 patients were randomised to laser PMR, and 12 patients to sham treatment; one of these was excluded from the MRI study due to a metallic CNS implantate. The LV anterior wall was treated in 7 laser and 4 sham patients, posterior wall in 5 respectively 6 and inferior wall in 3 respectively 6 of the patients. There were no significant differences between groups regarding age, AP class or history of previous myocardial infarction, diabetes or CABG. In the sham treated group there was one death in the first 24 hours following the treatment and one patient died after 2 months. Each patient was examined by MRI prior to the laser PMR, the day after PMR and finally 3 months after the laser PMR treatment. Each MRI study included cine GRE 2 chamber long axis (LA), 4 chamber LA, and 2 chamber short axis (SA) sequences covering the left ventricle (LV). Both perfusion and late enhancement studies were performed in a mid-LV SA slice, as a first pass respectively 15 min after iv injection of 0.05 mmol/kg bw of Gadolinium DTPA. The study parameters were wall thickening (WT), wall motion (WM), LV EF, LV end diastolic (ED) volumes, morphologic analyses, perfusion measured as peak signal intensity and time to peak intensity and delayed enhancement measured as signal intensity 15 min after contrast injection. When analysed, the LV was divided into 3 regions, anterior, posterior and inferior wall. All MRI data were analysed and evaluated while the treatment used still was double blinded. Data are presented as mean ± SD and t-test was used for statistical analyses.

Results: In the whole "BELIEF" study, 64 % of the patients in the laser group vs. 38 % in the sham group improved 1 or more angina class 6 months following treatment ($p < 0.01$). Prior to the PMR treatment there were no significant differences in the parameters measured between the laser and the sham treated groups. MRI the day after showed no visible signs of bleeding, pericardial effusion or any other complications due to the laser PMR. MRI did not detect myocardial channels after the PMR treatment. There were no significant differences in LV EF, in perfusion or in overall delayed enhancement after one day and 3 months. The increase in signal enhancement was the same for the laser group as for the sham group. Also, the delayed enhancement was the same (Table 1 & 2 on previous page).

Conclusion: In the whole "BELIEF" study, the symptoms of the laser treated patients improved significantly compared to the sham group. The results of the present MRI study did not show any improvement in myocardial perfusion, thus not giving any support for angioneogenesis following laser PMR. Increased scar formation in the treated area was not seen, as 3 months data did not show any significant difference in delayed hyper enhancement, LV muscle volume or LV EDV.

289. Use of Cine-MRI for Detection of Wall Motion Abnormalities Unrecognized by Harmonic Echocardiography

Dipan Shah,[1] Hani Salti,[2] David Mehlman,[2] Suhail Bahu,[2] Michele Parker,[2] Robert Judd,[2] Raymond Kim.[2] [1]*Northwestern University, 8107 Carriage Crossing, Chattanooga, TN, USA;* [2]*Northwestern University, 251 E. Huron Street, Chicago, IL, USA*

Introduction: Left ventricular wall motion analysis is commonly utilized in the assessment of patients with cardiac symptomatology. The most commonly used technique for assessment of regional wall motion is 2-dimensional echocardiography. Despite recent advances in harmonic echocardiography, a major limitation of its use in wall motion assessment is inadequate endocardial visualization. Recent advances in cine-MRI may have helped to eliminate the problem of limited visualization, and may improve the overall detection of regional wall motion abnormalities.

Purpose: The purpose of this study was to determine the extent of myocardium not visualized on routine harmonic echocardiography, and to determine the rate of unrecognized wall motion abnormalities.

Methods: We evaluated 60 patients who underwent a harmonic 2-D echocardiogram for clinical indications, and who also underwent true FISP cine-MRI within 30 days. The mean age of the cohort was 55.5 years; 35 patients had evidence of coronary artery disease based on angiography, a history of coronary revascularization procedure, or enzymatically documented myocardial infarction. Echocardiographic studies were segmented using the standard American Society of Echocardiography 16 segment model, and assigned a wall motion score on a 1–4 scale (1, normal; 2, hypokinesis; 3, akinesis; 4,

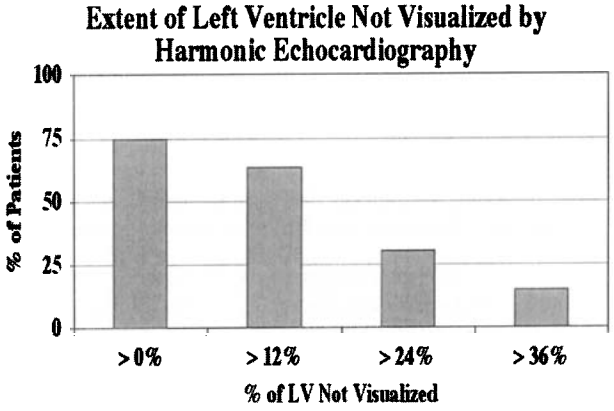

Figure 1.

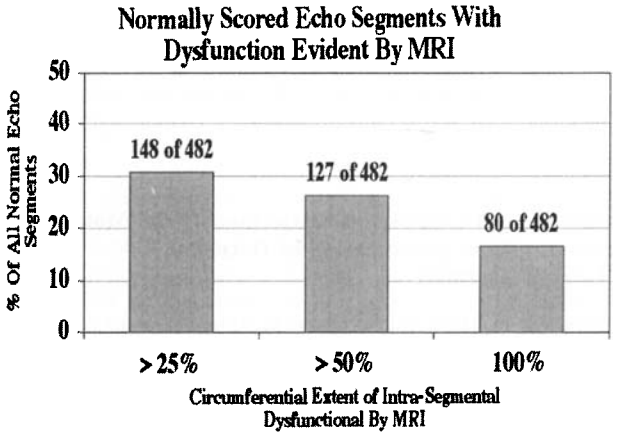

Figure 2.

dyskinesis). Each segment was also assigned an endocardial visualization score using a scale of 0–2 (0, not visualized; 1, poorly visualized; 2, adequately visualized). Cine-MRI studies were analyzed using a previously described 72-segment model and wall motion and endocardial visualization scores were assigned using the same scales. All studies were interpreted by a level 3 echocardiographer.

Results: Of 960 echocardiographic segments analyzed, 18% (171/960) were not visualized, 14% (132/960) were poorly visualized, and 68% (657/960) were adequately visualized. Adequate visualization of all echocardiographic segments occurred in 15 of 60 (25%) of patients (see figure 1). Of 4320 MRI segments, 99.9% (4314/4320) were adequately visualized. Cine-MRI provided adequate visualization of all segments in 98% (59/60) of patients.

Of the 788 echo segments which were visualized and graded for wall motion, 482 were scored as normal. Of these normal echo segments, 26% (127/482) were found to have dysfunction of at least half of their circumferential extent by cine-MRI (figure 2). A wall motion abnormality was detected in 75% (45/60) of patients with cine-MRI, compared to 63% (38/60) by echocardiography ($p < 0.04$).

Conclusion: Cine-MRI offers improved left ventricular endocardial visualization on a segmental and per patient basis. In addition, cine-MRI allows for significantly greater detection of wall motion abnormalities, possibly due to higher spatial resolution.

290. Contrast-Enhanced Magnetic Resonance Coronary Angiography Improves Resolution of Coronary Arteries

Henry Lucid,[1] Robert Biederman,[2] Walter Rogers.[3] [1]*Austin Heart, 511 Oakwood Blvd. Suite 100, Austin, TX, USA;* [2]*West Penn Allegheny Health System, 320 East North Avenue, Pittsburgh, PA, United States;* [3]*Allegheny General Hospital, 320 E. North Avenue, Pittsburgh, Pennsylvania, United States*

Introduction: A major advancement for Cardiology in the 21st century is the prospect of non-invasive coronary angiography. The most likely prospect for this seems to be achievable using Cardiac Magnetic Resonance Imaging techniques.

Purpose: This project was designed in an attempt to evaluate the possibility of improved coronary resolution and stenosis assessment using contrast-enhanced magnetic resonance coronary angiography. It is thought that the improved imaging characteristics of the Gadolinium enhanced images will result in better stenosis assessment both qualitatively to the observer's eye and quantitatively to the extent and location of the suspected occlusion. We also evaluated for improvement in the quality of the contrast and non-contrast images studies by calculating a signal to noise ratio (SNR) and contrast to noise ratio (CNR) for each contrast and non-contrast study.

Methods: The study population consisted of 30 consecutive female patients referred to the NIH WISE study for non-invasive assessment of suspected coronary artery disease chest pain syndromes. Each patient underwent non-contrast and contrast MRI coronary angiography. This population consisted of primarily patients with no prior history of coronary artery disease.

Imaging: Cardiac magnetic resonance imaging was performed on these patients using a Siemens 1.5T Magnetom whole-body imaging system (Siemens Medical Systems Iselin, N.J.) with the use of a phased array chest coil as the standard receiver. An axial 3D volume was positioned to cover the proximal coronary arteries with acquisition timed to late diastole. 1D data was acquired along the inferior and superior direction in the region of the right hemi-diaphragm. Data was saved only when diaphragm position was within a predefined $\pm$ 1 pixel window and the cardiac cycle was in late diastole. Image parameters included: 24 partitions, variable flip angle, band width = 244, centric k-space ordering, TR = 230ms, TE = 2.7ms, FOV = 250 × 250mm, 128 phase lines, 256 frequency lines. After acquisition of a 3D baseline set, infusion of 20ml of Magnevist contrast (Berlex Labs, Wayne NJ) was started at a rate of 0.1 ml/sec using an Spectris MR power injector (Medrad, Pittsburgh, PA).

MRI Analysis: Contrast and non-contrast studies were recalled from the computer storage disks in both random patient order and random imaging study order. The two blinded observers analyzed the data without any knowledge of the patients name, age, clinical history, or cath findings. A signal to noise ratio (SNR) and contrast to noise ratio (CNR) was determined for each contrast and non-contrast study. Each artery was graded on a scale of 0–3 (0 = not visible 1 = poor quality 2 = good quality 3 = excellent quality) as was the entire imaging sequence graded on the same 0–3 scale. The length of visible artery was recorded for each arterial vessel analyzed using the included Siemens MPR computerized manual drawing analysis software. When a flow void or suspected stenosis was found it was also graded on a 0–3 scale (0 = total signal loss or total occlusion 1 = markedly diminished signal or severe occlusion 2 = moderately diminished signal or moderate occlusion 3 = minimal diminished signal or minimal luminal irregularity). Both the length of occlusion and the distance from vessel origin were measured using the same computerized drawing analysis software.

Results: There was a statistically significant difference in the length of vessel visualized for the LM coronary artery

segment (1.08 ± 0.46 vs. 1.20 ± 0.60). There was a small non-statistically significant trend toward better visualization of the LAD (5.79 ± 1.59 vs. 5.89 ± 1.40), but not for the LCx (4.24 ± 1.53 vs. 3.82 ± 1.43) or RCA (2.98 ± 1.00 vs. 2.96 ± 1.17) segments. The intraobserver variability of those measurements was not significant for any of the four coronary artery segments analyzed. The SNR and CNR calculated for each of the contrast and non-contrast studies revealed that the SNR (1.5 ± 0.1 vs. 1.1 ± 0.2) was statistically higher in the contrast studies as was the CNR (1.4 ± 0.2 vs. 1.0 ± 0.1). Stenosis assessment using this k-space aquisition method was found to be inadequate. The low prevalence of disease in the population did not allow for statistical analysis of the assessment of coronary artery stenosis, and the apparent low sensitivity of the test within that small population makes it appear that this technique would not be effective.

Conclusion: The findings of this study are less impressive, but consistent with prior MR coronary angiographic studies. The more proximal portions of the vessels and the technically easier to visualize vessels (LM and LAD) are imaged adequately with this modality. The main problems, aside from technically inadequate visualization in 10–15% of vessels segments, are with tapering of the distal segments that tend to fall out of the imaging fields of view and the location of the RCA and Cx in the more posterior portions of the heart further from the receiver coil. These results parallel others findings most likely because of MRI's enhanced ability to visualize the proximal coronary artery segments and the location of the RCA and Cx in the more posterior portions of the heart further from the receiver coil. The use of an intravascular contrast agent in this study had the effect of improving the resolution and visualization of the coronary artery segments analyzed. The potential for newer and better contrast agents may lead to better visualization in the future. Gradient strength has played an important role in the development of this imaging technology. As the gradients get stronger and the computers and software used to drive them improve, one would expect an improvement in the signal and resolution. Additionally, newer coil designs that collect several lines of k-space data simultaneously, spiral k-space acquisition, will decrease image acquisition time. The combination of these advancements will certainly lead Cardiac MRI of the coronary arteries to the clinical forefront in the years to come.

291. Comparison of Atrioventricular Plane Displacement in Subendocardial Versus Transmural Myocardial Infarction Using Magnetic Resonance Imaging

Chun Chiu,[1] Nina So,[1] Wynnie Lam,[1] Anna Chan,[1] Yan Zhang,[1] John Sanderson.[1] [1]*Prince of Wales Hospital, The Chinese University of Hong Kong, Shatin, Kowloon, Hong Kong, SAR*

Introduction: Atrioventricular plane displacement (AVPD) is though to reflect the function of subendocardium, which composed mainly of longitudinal muscle fibers. Abnormalities in long axis systolic function reflected by AVPD have been documented in myocardial infarction. Contrast magnetic resonance imaging (MRI) can detect and quantify subendocardial and transmural infarcts. We used MRI to measure AVPD and infarct size and explored the differences between subendocardial and transmural infarct.

Methods: Contrast MRI was performed with Siemens Sonata System using intravenous Gadolinium-DTPA at a dose of 0.2 mmol/kg. After 15 minutes, images were acquired with the use of a segmented inversion-recovery (IR-FLASH) sequence. 7 patients with subendocardial infarction as defined by < 50 % thickness of hyperenhancement was matched with 7 patients with full thickness transmural infarct with comparable infarct size estimated by longitudinal length. True FISP cine images were created at the 4 chambers and 2 chambers views similar to echocardiography. Straight lines were drawn form the apex to the attachment of the mitral valve at both 4 chamber and 2 chamber views- the difference between systole and diastole reflected the AVPD. The extent of displacement was measured in the septal, lateral, posterior and anterior regions corresponding to the sites of the infarcts.

Results: The site of infarct were anteroseptal n = 3, inferior n = 2 and lateral n = 2. There was no difference between the 2 groups in terms of estimated infarct size: the average longitudinal infarct length divided by the length of the long axis of the left ventricle was 0.48 cm in the subendocardial infarct group versus 0.50 cm in the trasmural infarct group (p = 0.26 NS). The corresponding AVPD in the subendocardial infarct group was 0.80 cm (SD 0.35) and in the trasmural infarct group was 0.81 cm (SD 0.49), p = 0.94 NS.

Conclusion: We found that there was no significant difference in long axis systolic function as reflected by AVPD in patients with subendocardial infarct versus transmural infarct. Our results support the hypothesis that AVPD reflects subendocardial function and is affected to the same extent in subendocardial and transmural infarctions

292. Three-Dimensional Free-Breathing Imaging of Myocardial Infarction

Susan Yeon,[1] Matthias Stuber,[1] Kraig Kissinger,[1] Franz Aepfelbacher,[1] Peter Danias,[1] Abhishek Gaur,[1] Warren Manning.[1] [1]*Beth Israel Deaconess Medical Center, Cardiovascular Division, Boston, MA, USA*

Introduction: Among patients with coronary artery disease, the presence and size of myocardial infarction (MI) has important prognostic and therapeutic implications. MI location and extent has previously been characterized by delayed myocardial contrast hyperenhancement using a breath-hold 2D segmented inversion-recovery MR pulse sequence. Complete left ventricular assessment requires imaging at multiple levels and orientations. However, patients with significant left ventricular dysfunction who are most likely to benefit from such analysis are frequently unable to perform multiple breath holds due to cardiovascular or coexistant pulmonary disease. The use of a navigator to suppress respiratory motion would enable volumetric left ventricular assessment during free-breathing.

Purpose: To develop a 3D navigator gated free-breathing protocol to detect myocardial hyperenhancement for assessment of prior MI.

Figure 1.

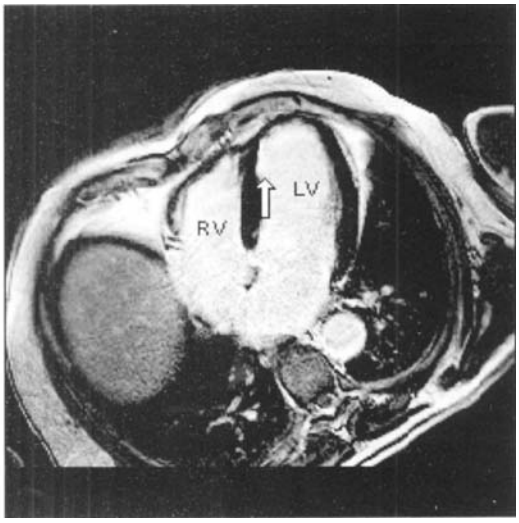

Figure 3.

Methods: A free-breathing 3D acquisition using an inversion recovery T1-enhanced turbo field echo (spoiled segmented gradient echo) pulse sequence was implemented on a 1.5 T Philips Gyroscan ACS-NT system with a 5-element cardiac synergy coil. Vector ECG was used for triggering on every other cardiac cycle to provide adequate time for T1 relaxation. Contrast enhanced images were acquired 10–20 minutes following intravenous administration of 0.2 mmol/kg Gd–DTPA (Magnevist®, Berlex Laboratories). An inversion time of 225–275 ms was selected to minimize signal from normal myocardium. A real-time navigator was used to gate respiratory motion (5 mm gating window) and to prospectively correct for motion in the cranial–caudal direction. The imaging sequence included a TR of 5 msec, TE of 3 msec, flip angle of 15°, and acquisition window of 298 msec. The field of view was 330 mm with a 256 × 256 scan matrix. One or two signal averages were acquired. An 8–10 cm thick slab was imaged consisting of 2 stacks of 8–10 slices, each 5 mm in thickness. Images were obtained at 16–20 left ventricular short-axis levels, at 8–10 levels parallel to the four-chamber orientation, and at 8–10 levels parallel to the two-chamber orientation. We studied 8 subjects with left ventricular systolic dysfunction and known or suspected coronary artery disease including seven patients with known prior MI.

Results: The imaging protocol was completed in 7 subjects. Total scan time for each slab was ~ 2 minutes. In one MI subject with large bilateral pleural effusions the protocol was prematurely terminated due to orthopnea. Regions of hyperenhancement consistent with MI were detected in all 6 patients with a clinical history of MI. No hyperenhancement was found in one patient with non-ischemic cardiomyopathy. Figure 1 shows a 2-chamber long-axis view of the left ventricle with a nearly transmural hyperenhancing region in the inferior wall of the left ventricle. Figure 2 shows three short-axis levels (apical to basal) of the left ventricle in the same subject demonstrating the distribution of the inferior MI in this orientation. Figure 3 demonstrates a 4-chamber long-axis view of the left ventricle in another subject with hyperenhancing distal septal and apical subendocardial segments.

Conclusion: Acquisition of a 3D data set provides full spatial mapping of the location, extent, and depth of MI. Implementation of a navigator for respiratory motion tracking permits collection of 3D data in a free-breathing state, thus potentially improving both SNR and the applicability of this approach to clinical populations.

Figure 2.

293. Non Invasive Assessment of Regional Myocardial Perfusion in Patients with Coronary Artery Disease: Qualitative and Quantitative Contrast-Enhanced Magnetic Resonance vs Contrast Echocardiography

Patricia Iozzo,[1] M. Aurora Morales,[1] Daniele Rovai,[1] Alessia Gimelli,[1] Vincenzo Positano,[1] Paolo Marcheschi,[1] Martha Morelos,[1] Olaf Rodriguez,[1] Massimo Lombardi.[2]
[1]*National Research Council, Via Moruzzi 1, Pisa, Italy;* [2]*IFC - National Research Council, Via Moruzzi 1, Pisa, Italy*

Introduction: The non-invasive assessment of regional myocardial perfusion, using imaging techniques that do not involve ionizing radiation, such as magnetic resonance and echocardiography is under investigation.

Purpose: Aims of the present study were: a) to evaluate the potential role of two non-invasive techniques, namely contrast-enhanced magnetic resonance imaging (MRI) and contrast echocardiography (MCE), in the assessment of myocardial perfusion; b) to investigate whether semiquantitative analysis would improve the accuracy of myocardial perfusion measured with MRI.

Methods: Ten patients with previous myocardial infarction and regional wall motion abnormalities were included in the study. MCE was performed with a commercial scanner (GE-Vingmed System 5), implemented with harmonic power Doppler, triggering at end-systole every 2 cardiac cycles. Apical 4 and 2 chamber views were obtained during i.v. injection of a bolus of Levovist followed by a slow infusion (4 grams in 3 minutes, 400 mg/ml). MRI was conducted with a CVi 1.5 Tesla magnet (GE), using an ECG-triggered FGR/ET sequence during first pass of an i.v. bolus of gadodiamide (Omniscan). A home made software package was used to obtain absolute and relative slope/peak measures. Values of relative slope in excess of 45% were excluded from analysis because of possible contamination from the LV chamber. Results from 8 patients were also compared with those obtained from myocardial SPECT.

Results: The number of segments visualized were 160/160 with MRI, 150/160 with MCE, and 127/128 with SPECT. Visual inspection resulted in a fair agreement of MRI vs both MCE and SPECT, and in a moderate agreement between MCE and SPECT. Based on simple regression between visually observed and calculated values of MRI perfusion, absolute ($p = 0.037$) and relative ($p = 0.017$) slopes were judged as the more appropriate parameters for comparison. A significant correlation was found between relative slope values and SPECT estimates ($p = 0.029$).

Conclusion: We conclude that: a) compared with MRI, MCE appears to offer a slightly greater concordance with SPECT when visual inspection analysis is employed; b) MRI has the dual advantage of guaranteeing complete visualization of all LV regions, and of being operator independent; c) preliminary quantitative results of myocardial perfusion by MRI seem to improve its accuracy and support further investigation in this direction.

294. Coronary Artery Motion in Patients with Coronary Artery Disease (CAD): Implications for the Timing of Image Acquisition in Coronary MR Angiography

Salil Patel,[1] John Oshinski,[1] Amy Whigham,[1] Alex Hakim,[1] Mark E. Leimbach,[1] Roderic Pettigrew.[1]
[1]*Emory University, Radiology Department, Atlanta, Georgia, United States*

Introduction: Coronary artery motion during image acquisition is a limiting factor in the development of coronary MR angiography. In order to minimize the effects of coronary motion, MR angiography should be performed during those parts of the cardiac cycle when coronary motion is minimal.

Purpose: Current practice in coronary MR angiography is to acquire images in diastole, typically from 55–70% of the cardiac cycle. A study using data from electron-beam CT suggests that imaging should occur much earlier in the cardiac cycle, at 30–50% of the cycle. Other studies have shown that the RCA moves greater than the LAD and LCX, but the precise 3D-motion of the coronary arteries throughout the cardiac cycle is not well characterized. The purpose of this study was to quantitatively analyze the motion of the coronary arteries using both cardiac catheterization angiography and ECG-gating data. Motion analysis was used to identify and characterize periods of relative coronary motion quiescence.

Methods: Digital-archived ECG-gated bi-plane angiography films on 15 patients with CAD were reviewed. Two orthogonal planes were evaluated for each coronary. Landmarks on the proximal, mid, and distal points of all three of the coronary arteries (RCA, LAD, LCX) were identified and their position was tracked over the cardiac cycle. Displacement between successive frames was determined for each landmark over the cardiac cycle. Frame-to-frame displacement was measured in three perpendicular directions, and three-dimensional displacement was calculated. The location and duration of periods when frame-to-frame displacement was < 1 mm were identified. Cardiac cycle timing was defined as starting at the first QRS complex (0%) and finishing at the next QRS complex (100%).

Results: RCA displacement was up to 2.8 times and 2.9 times greater than the LAD and LCX, respectively. RCA displacement averaged 1.5 times greater than the LAD and LCX. All three coronaries had two periods of relatively low motion (see figure).

The first period occurred after completion of ventricular systole, at 30–40% of the cardiac cycle, when all three vessels had frame-to-frame displacement <1.5 mm. This first period

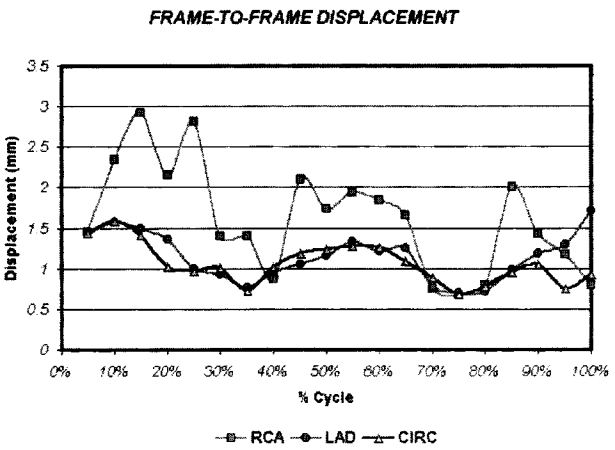

Figure 1.

lasted 50–100 ms. The second period occurred after relaxation of the ventricles, from 70–85% of the cardiac cycle, when all three vessels had frame-to-frame displacement <1.0 mm. This second period was also longer than the first period, lasting at least 100 msec (range 100–150 ms). The timing of this second period was in mid-diastole, but varied among patients (76 ± 5% of the cardiac cycle). Frame-to-frame displacement increased at end-diastole during atrial systole.

Conclusion: This study quantitatively describes the motion of the coronary arteries. The RCA motion is up to 2.9 times greater than vessels in the left system. While coronary motion is present throughout the cardiac cycle, including end-diastole, all patients have two periods where all 3 arteries have relatively little motion. The first period occurs immediately after ventricular systole, but it is relatively short (50–100 ms). Another period of relative quiescence occurs in mid-diastole, rather than end-diastole, and lasts 100–150 ms. This period also has a lower mean frame-to-frame displacement (0.8 mm) than the first period (1.0 mm). Timing of MR angiography to acquire images during this period in mid-diastole should result in image quality least affected by motion.

295. Fast Navigator-Gated Coronary MRA with Individualised Acquisition Window and Motion Adaptive Gating

Sven Plein,[1] Tim Jones,[1] John Ridgway,[2] Mohan Sivananthan.[1]
[1]*Leeds General Infirmary, Gt. George Street, Leeds, West Yorkshire, United Kingdom;* [2]*Leeds Teaching Hospitals, Department of Medical Physics, Leeds, West Yorkshire, United Kingdom*

Introduction: Free-breathing MR Angiography (MRA) with respiratory navigators allows acquisition of high-resolution three-dimensional data sets of the coronary arteries, but the scan times of navigator gated MRA are long. The reasons for this include: 1) Fixed acquisition windows based on the heart rate are generally used in MRA, which do not account for the considerable variability of the coronary motion between individuals. As a consequence, acquisition windows have to be short to avoid image blurring. Assessing the coronary motion in each patient individually may allow the use of longer acquisition windows and thus shorten scan times. 2) The efficiency of respiratory navigators is often low because narrow gating windows are required to reduce the motion artefacts to acceptable levels and drifting of the mean end-expiratory diaphragm position can occur in long acquisitions. Adaptive gating windows may improve navigator efficiency and maintain or improve image quality, because in adaptive gating the central parts of k-space are acquired with a narrow acquisition window and the outer parts with a wider acquisition window. A high proportion of the data is therefore acquired with a wide window, at higher navigator efficiency, but the important contrast information is acquired with a narrow window.

Purpose: The aim of the study was to investigate if scan times in navigator gated MRA can be shortened by the combination of individually determined acquisition windows and adaptive gating.

Methods: 25 patients with known or suspected CAD who were scheduled for x-ray angiography were included in the study. Patients had an MRI examination on a 1.5T Philips INTERA CV system (Philips Medical Systems, Best, The Netherlands). To determine the best acquisition window for each patient, we acquired a breath hold cine scan in the four-chamber orientation with high temporal resolution (Balance Fast Field Echo = BFFE, TR 2.8 ms, TE 1.4 ms, flip angle 55°, 30 phases per cardiac cycle). From this the motion of the right (RCA) and the left coronary arteries in the cardiac cycle was assessed and the time of minimal coronary motion assessed for each vessel. The position of the coronary arteries was planned form a coronary scout (3D segmented-EPI, TR 16 ms, TE 4.9 ms, flip angle 40°, 50 slices of 2 mm thickness) with a 3-point planscan tool. 3D data sets of the RCA and the left system were acquired separately. Coronary MRA was performed with a 3D segmented k-space gradient echo sequence with real-time navigator on the right hemidiaphragm (TR 7 ms, TE 2.1 ms, flip angle 25°, T2 preparation and fat suppression prepulses, magnetization transfer, spatial resolution 1.04 × 0.78 × 1.5 mm, 16 slices, respiratory navigator gating and tracking with real time correction in the cranio-caudal direction). The acquisition window and trigger delay were set individually for each patient according in the period of minimal coronary motion determined from the high temporal resolution cine. During data acquisition, an adaptive gating window was used for the real-time navigator with a 2 mm window for the central 35% of k-space and 6 mm for the outer 65% of k-space. We also allowed continuous correction of the mean gating window position to adjust for diaphragmatic drift during the acquisition.

Images were read by two observers who were blinded to the results of the x-ray angiogram. The presence of significant coronary stenoses in each vessel was reported by consensus between the observers. The results were compared with the

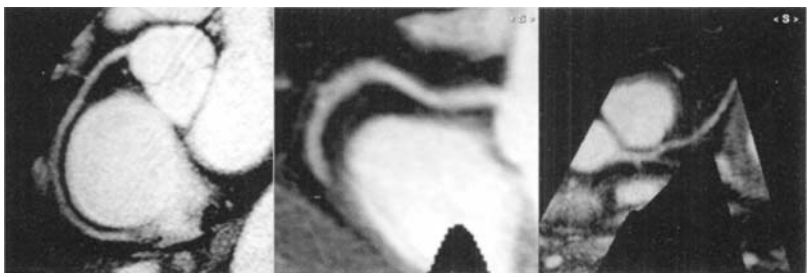

Figure 1.

x-ray angiograms and the sensitivity and specificity of MRA to detect coronary stenoses >70% was calculated.

Results: The acquisition window determined from the high temporal resolution cine ranged from 140 and 200 ms and trigger delays varied between 450 to 800ms. The image quality of the acquired data was sufficient for analysis in 47 of the 50 data sets. In three data sets, images were degraded due to respiratory motion artefacts. The mean scan time was 4.3 (± 1.2) min per coronary data set and the mean navigator efficiency was 46.3% (± 13.9). The sensitivity to detect significant coronary artery disease compared with x-ray angiography was 85.1% with a specificity of 71.4%. Figure 1 gives examples of coronary data sets acquired in this study.

Conclusion: With the sequence presented, 3D coronary data sets were acquired with an approximately 4-fold reduction in scan time compared with previously described navigator gated MRA sequences (1). This was achieved by using longer acquisition windows, which were determined individually for each patient. We used an easy and practical approach to determine the time of minimal coronary motion, which only requires a single additional 8 second scan. In addition, by using adaptive gating and continuous gating level correction, we achieved high navigator efficiencies in a group of clinical patients and image quality was good in the majority of data sets. The diagnostic accuracy of this approach was similar to published data (1). A comparison of this approach with other navigator-based techniques should now be undertaken.

296. Quantitative Perfusion Analysis of Contrast-Enhanced MRI

Dara Kraitchman,[1] Nicole Holloway,[2] Raymond Boston.[3]
[1]*Johns Hopkins University, JH Medical Institutions E Balt, Baltimore, Maryland, United States;* [2]*Johns Hopkins University, 601 N. Caroline St., Baltimore, MD, USA;* [3]*University of Pennsylvania, School of Veterinary Medicine, Kennett Square, PA, USA*

Introduction: There has been much debate over the source of overestimation of infarction size by delayed hyperenhancement MRI relative to post-mortem measurements (e.g., TTC staining). Recently, Thornhill and co-workers have shown no difference in partition coefficient in stunned canine myocardium [1]. Other canine studies have failed to demonstrate hyperenhancing patterns in stunned myocardium [2] giving credence to the hypothesis that the overestimation of infarct size by MRI may be due to partial volume effects.

Purpose: In this study, we investigated whether quantitative analysis of first-pass contrast-enhanced MRI yielded parameters with different values in stunned canine myocardium relative to normal myocardium.

Methods: Five mongrel dogs (20–25 kgs) were subjected to a 20-minute closed-chest left anterior descending coronary artery occlusion via cardiac catheterization followed by reperfusion to create myocardial stunning without myocardial infarction. Each dog was imaged several days prior to cardiac catherization (baseline), in the first hours after reperfusion (stunning), and at one week after reperfusion (recovery) under general inhalational anesthesia. All animals were imaged in a 1.5 T MR scanner (CV/i, GE Medical Systems, Milwaukee, WI). First-pass contrast-enhanced images were acquired using an ECG-gated, breath-hold, interleaved, saturation recovery, gradient-echo, echoplanar pulse sequence (EFGRET-ET) after a bolus injection (5 cc/s, Medrad, Indianola, PA) of Gd–DTPA (0.05 mmol/kg iv) for 40–50 cardiac phases. Imaging parameters were: 28 × 21 cm FOV; TR/TE/TI=6.2/1.2/160 ms; 128 × 128 image matrix; 8 mm slice thickness; 4–6 slices;125 kHz BW; 20° FA; and ETL = 4.Regional myocardial blood flow (RMBF) was determined by radioactive microspheres at each imaging session and during coronary occlusion. Viable myocardium was determined post-mortem by TTC staining.Signal intensity versus time curves (STC) were determined using a custom software package (cine, GEMS) in 6 myocardial ROIs per imaging slice and the left ventricle. The left ventricular STC was used as an input function to a two compartment model. The fractional turnover rates (FTR) into and out of the myocardium in each ROI were determined in by fitting the model using the winSAAM compartment modeling software [3]. Over 200 ROIs were fitted at baseline, stunning, and recovery. Statistical testing for differences between baseline, stunning, and recovery was performed using a multivariate analysis of variation with correction for repeated measures (Stata, Stata Corporation, College Station, TX).

Results: Coronary occlusion of 20-minutes resulted in stunned myocardium without myocardial infarction based on TTC staining. After reperfusion, RMBF was restored in all animals. FTR into and out of the myocardium did not differ between baseline and recovery in any ROI (P = NS). FTR into and out of the myocardium in both the stunned and non-stunned ROIs were significantly different than baseline and recovery ($P < 0.001$, Table). The ratio of FTR into and out of the myocardium was increased at stunning relative to baseline and recovery. However, no hypo- or hyper-enhancement was observed in either the stunned or nonstunned myocardium at any imaging session.

Conclusion: Using a low-dose contrast injection, we were able to determine quantitative parameters of wash-in and wash-out (FTR). Visual assessment did not reveal any changes in enhancement of stunned myocardium relative to normal

Table 1

Fractional Turnover Rates

	Baseline	Stunning	Recovery
Into myocardium (wash-in)	0.08 ± 0.02§	0.10 ± 0.04	0.15 ± 0.08§
Out of myocardium (wash-out)	0.19 ± 0.11§	0.23 ± 0.14	0.35 ± 0.16§

non-stunned tissue. FTRs were altered immediately after myocardial stunning in both stunned and normal tissue. While regional myocardial blood flow (determined by radioactive microspheres) was restored, alterations in regional blood volume due to inflammatory mediators released early after reperfusion and transient cellular swelling in stunned but viable tissue may account for the alterations in FTR observed globally in the early hours after ischemia injury but not at one-week when stunned myocardium had recovered.

297. The Use of CMR Measured Cardiac Function and Perfusion Indices to Predict Outcome as a Function of Coronary Artery Stenosis Level

Mark Doyle,[1] Robert Biederman,[2] Anthon Fuisz,[3] Sheryl Kelsey,[4] Delia Johnson,[4] Eduardo Kortright,[5] Edward Walsh,[1] Barry Sharaf,[6] Lindsey Tauxe,[1] William Rogers,[1] Noel Bairey Merz,[7] Gerald Pohost.[1] [1]*University of Alabama at Birmingham, D201G, Diabetes Building, Birmingham, Alabama, United States;* [2]*West Penn Allegheny Health System, 320 East North Avenue, Pittsburgh, PA, United States;* [3]*Washington University, 555 Washington, Washington, DC, USA;* [4]*University of Pittsburgh, A543 Crabtree Hall\130 DeSoto Street, Pittsburgh, Pennsylvania, United States;* [5]*University of New Orleans, UNO Math Dep, New Orleans, LA, USA;* [6]*Rhode Island Hospital, RHI Hspital, Providence, RI, USA;* [7]*Cedars-Sinai Research Institute, CSRI, Los Angeles, CA, USA*

Introduction: It has been demonstrated that severity of coronary artery stenoses detected by coronary angiography are poor predictors of cardiac events. Recently, we showed that CMR derived measurements of a global myocardial perfusion (GMP) index and ejection fraction (EF) were independent predictors of cardiac events. We hypothesize that the use of the GMP index and EF at different levels of coronary stenosis can predict observed event rates.

Purpose: To use the CMR derived global myocardial perfusion index and EF levels to determine the predictive value of coronary artery stenosis level. The significance of this is that patients with low grade coronary artery stenosis may be at risk for thrombotic events (e.g. by rupture of vulnerable plaque), and patients with high grade stenosis may be at risk for infarction due to progressive occlusive disease. The ability to assess the nature of the risk from the level of stenosis determined by coronary angiography would be of great clinical value in patient management and could lead to improved survival.

Methods: 124 women (age 59 ±11 yrs) enrolled in the NHLBI Women's Ischemia Syndrome Evaluation (WISE) were studied using first pass CMR perfusion and EF. A GMP index was calculated for two cardiac short axis views by the following method. The time-intensity curve for each of 12 myocardial regions was characterized by a linear slope and the net signal increase from baseline to peak intensity. The slope parameter for each region was normalized by dividing it by the input slope for the left ventricular blood pool. The area under the triangle formed by the normalized slope and the net signal increment from baseline to peak intensity was calculated to form the myocardial perfusion index. This index was averaged over the 12 myocardial territories to form the GMP index. The GMP index was measured under hyperemic conditions (using 0.56 mg/kg of dipyridamole infused over four minutes).

The EF was generally calculated from the multiple slice short axis views. When these were technically inadequate, the two long axis cine views were used. The GMP index and EF were categorized into four groups (quartiles). The quartiles of both variables were summed to form a combined left ventricular (LV) function index, range 2 to 8, with 2 representing patients in the lowest quartile of both parameters and 8 indicating the highest quartile of both parameters.

Coronary angiography was performed within one day of the CMR examination. Quantitative coronary analysis was conducted at the WISE core laboratory and the maximum level of stenosis noted. Maximum stenosis levels were grouped into deciles. Women were followed for events (cardiac death, myocardial infarction or hospitalization for angina) at 6 weeks and at yearly intervals (28 ± 7 months).

Results: There were 26 events (21%). When analyzed by Kaplan Meier survival analysis, a decreasing LV function index showed a significant trend towards a higher event rate (log rank = 22.4, $p = 0.001$). There were no events in patients in the highest two categories of LV index (n = 18, 15%). However, the average maximum stenosis level of the these two LV function index categories was not significantly different from the lower five categories (average maximum stenosis level 34% vs 31%, $p = 0.73$).

Kaplan Meier survival analysis performed on the deciles of maximum coronary artery stenosis, demonstrated a weak trend to increasing rate with increasing stenosis level (log rank = 8.6, but an insignificant p value of 0.28). When the lowest risk patients as assessed by LV index (the two highest groups) were excluded, and Kaplan Meier survival analysis performed on the remaining patients grouped in deciles of maximum stenosis, the log rank statistic increased to 15.9 and achieved statistical significance, $p = 0.03$.

Conclusion: The degree of coronary artery stenosis detected by angiography has been shown to be a poor predictor of cardiac events. CMR can provide myocardial perfusion indices and measurements of EF that are predictive of cardiac events. When excluding patients based on high values of both myocardial perfusion and EF, the remaining patients demonstrate a linear trend of increasing event rate with increasing stenosis level. It is apparent that coronary artery stenosis level becomes a risk factor in those patients identified by CMR to be at risk. Thus, the CMR LV function index permits risk stratification based on coronary artery stenosis level. Correct risk assessment and knowledge of the level of coronary artery stenosis could lead to the ability to differentiate an outcome between plaque rupture vs progressive occlusive disease. Accordingly, the CMR LV index may allow improved patient management.

298. Real-Time SENC for the Detection of Regional Dysfunction During Dobutamine Stress Test

N.F. Osman,[1] S. Sampath,[1] J.A. Derbyshire,[2] E. Castillo,[1] D. Bluemke,[1] E. Zerhouni,[1] J.L. Prince,[1] D. Kraitchman.[1] [1]*Johns Hopkins University, Baltimore, MD, USA;* [2]*National Institutes of Health, NHLBI, LCE, Bethusda, HD, USA*

Introduction: Despite the tremendous potential of cardiac MRI stress testing, the need for fast imaging with adequate spatial resolution to detect wall motion abnormalities remains a challenge that hampers its clinical application. Because long imaging times with breath holding are needed to produce high-resolution images, patient monitoring during increasing doses of pharmacological stress is often difficult [1]. Recently, fast imaging sequences have been developed to produce real-time movies of the contracting heart without breath-holds [ref]. These real-time sequences often have significant image degradation due to the low spatial resolution and motion artifacts created by free breathing. The blurring of the endocardial and epicardial wall boundaries can hinder the detection of wall thickening abnormalities.

Purpose: We propose combining strain-encoded (SENC) imaging [2] with fast sequences to provide a semiquantitative method to detect changes in segmental contractility. SENC applies a 1-1 SPAMM pulse sequence at end-diastole to encode the tissue with a sinusoidal pattern in a direction orthogonal to the imaging plane. Deformations of tissue during systole change the local frequency of the pattern in proportion to the through-plane strain component. A modified imaging sequence produces strain-encoded images, whose intensity distribution reflects local frequency; hence, the through plane, contractility. The SENC method therefore produces images where the regional dysfunction accompanying an ischemic event is manifested as regional hypointensity (or hypointensity).

Methods: The imaging algorithm for real-time SENC consists of combining the SENC method with fast imaging sequences for free-breathing imaging, whereby a low-resolution SENC image can be created to detect motion abnormalities and thus ischemia in a semi-automated manner. To demonstrate this, we acquired a full image with a resolution of 2 mm. The low-resolution images were produced from the original image by filtering the images with a low-pass filter to undersample the phase-encoding lines during fast imaging.

Results: Figure 1 shows the SENC images for different resolutions in the y direction. The rows represent 256, 80, and 48 lines of phase encodings. The columns represent the low tuning frequency, high tuning frequency, and the circumferential strain. The blue strain color indicates contraction while red indicates no contraction (or minor stretching). The red region, indicated by the arrow, is an area of experimentally-created myocardial stunning in a dog. While the reduction in the number of the phase-encoding views caused blurring of the acquired images, the dysfunctional regions are immediately apparent. Potentially, if the undersampled phase-encoded images (middle and lower row of Figure 1) were acquired directly, motion artifacts may be reduced.

Notice that the resolution of the resulting strain maps equals the size of the pixels of the acquired image. Hence, if the resolution is decreased until only three pixels cover the wall thickness, it will still be sufficient to detect the difference in transmural contractility, *i.e.*, between sub-epicardium, midwall, and sub-endocardium.

Conclusion: We suggest that the occurrence of an ischemic event can be easily detected (in a semiquantitative manner) in a strain-encoded image despite the low image quality. This will enable the assessment of regional function and the detection of the onset of ischemia during a stress test. In addition, the decreased imaging time with real-time SENC will enable the determination of motion abnormalities at the high heart rates that often occur at high doses of physiologic stress. Thus, real-time SENC has the potential to providing an invaluable tool for monitoring a patient inside the MR scanner.

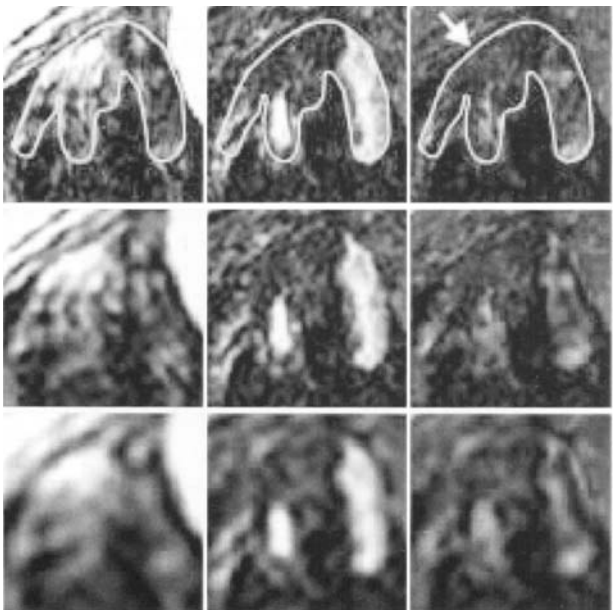

Figure 1.

299. Delayed Enhancement Volumetric Imaging of the Entire Left Ventricle in a Single Breath-Hold Using Sensitivity Encoding (SENSE)

Kamal Gupta,[1] Raja Muthupillai,[2] Vei Vei Lee,[3] Scott D. Flamm.[1] [1]*St. Luke's Episcopal Hospital/Texas Heart Institute, 6720, Bertner Avenue, MC 2-256, Houston, Texas, USA;* [2]*Philips Medical Systems, St. Luke's Episcopal Hosp./Radiology/MRI, Houston, Texas, United States;* [3]*Texas Heart Institute, Department of Biostatistics, Houston, TX, USA*

Introduction: Delayed enhancement (DE) imaging following Gd-DTPA administration has been shown to identify regions of irreversible myocardial injury(1,2). Hitherto described DE techniques acquire a single slice per breath-hold requiring several breath-holds to assess myocardial injury over the entire left ventricle (LV) (1,2). We have developed a volumetric DE method that covers the entire LV in a single breath-hold using SENSE (or in two breath-holds without SENSE).

Purpose: The purpose of the study is two fold. First to describe the development of a 3D DE technique that can cover the entire LV over a single breath-hold. Second to test the feasibility of using this technique in patients for evaluation of myocardial injury using quantitative and qualitative measures over conventional 2D DE techniques.

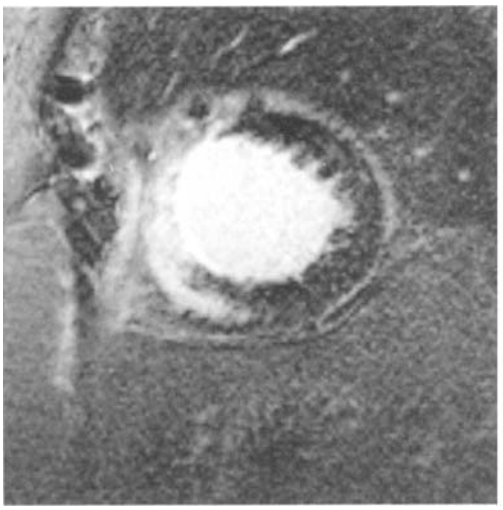

Figure 1. 2D DE technique.

Methods: In 19 patients (13 male, 60 ± 13 years, 12 with areas irreversible myocardial injury and 7 with no injured myocardium), conventional 2D DE technique was compared against the 3D DE technique with and without using SENSE on a 1.5T Philips Intera (Rel 7.1.x/8.1.x). In an ECG gated, inversion-recovery TFE sequence, following a 180° pulse, a set of gradient echoes were collected in diastole. The acquisition parameters for each technique were as follows:

2D DE: TR/TE/flip/views per RR/acq. time = 6.8/2.1/15°/32/16 heart beats (hb) per slice.

3D DE (No SENSE): TR/TE/flip 3.5/1.12/15°; views per RR 55/16 hb for 5 slices; 2 breath-holds to cover the entire LV.

3D DE SENSE: TR/TE/flip 3.5/1.2/15°; views per RR 55/22 hb for 10 slices. The number of in-plane phase

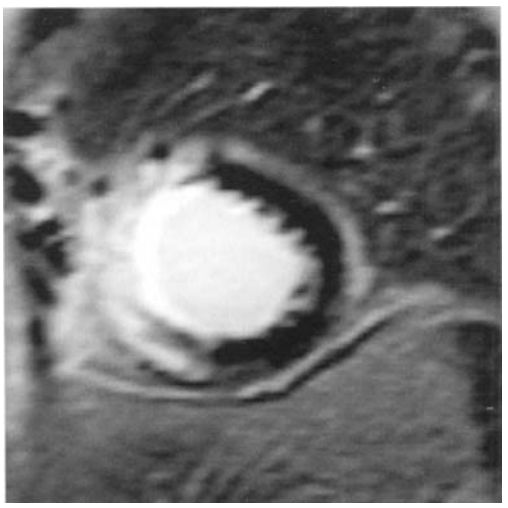

Figure 2. 3D DE (without SENSE) technique.

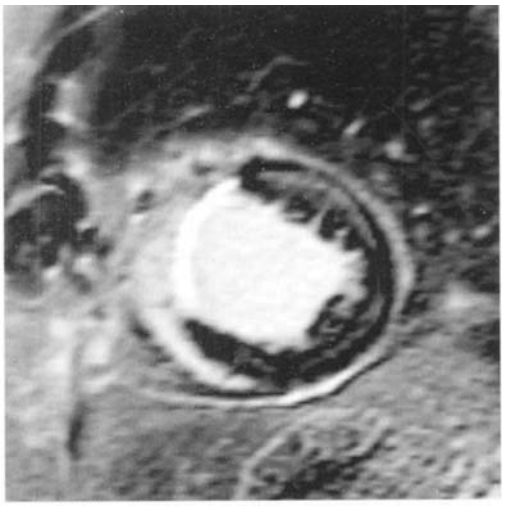

Figure 3. 3D DH technique with SENSE.

encoding steps was reduced by a factor of 2, and a radial ky-kz profile order was used for the SENSE acquisition. The same FOV and slice thickness were maintained for all three techniques; acquired matrix sizes were 256 × 256 for 2D, and 208 × 208 for the 3D techniques. The techniques were quantitatively evaluated using Contrast-to-Noise Ratio (CNR) between normal myocardium and injured myocardium (Inj-Myo), injured myocardium and blood-pool (Inj-Bl), and blood-pool and normal myocardium (Bl-Myo) for all three techniques, and qualitatively evaluated for misregistration artifacts.

Results: Images from the three techniques are shown in Figures 1–3. There was no statistically significant difference in Inj-Myo CNR between the 2D and 3D techniques, and between the two 3D techniques. For Inj-Bl CNR, the difference between the 2D and 3D technique was statistically insignificant, however the single-breathhold 3D SENSE was better than the 3D without SENSE ($p < 0.004$); for Bl-Myo CNR, the difference between the two 3D techniques, and between the 2D and 3D (without SENSE) was statistically insignificant, however the difference between 3D SENSE and 2D was statistically significant ($p < 0.002$)with the former being better. Qualitatively, there were misregistration artifacts in 31% of patients due to inconsistent breath-holding in the 3D technique without SENSE.

Conclusion: Our results show that the single breath hold 3D DE technique using SENSE is clinically feasible. When compared to the currently used 2D methods, the 3D SENSE DE technique provides equivalent contrast between the injured and normal myocardium, and better contrast between normal myocardium and blood pool. In addition, the 3D SENSE technique eliminates misregistration caused by inconsistent breath-holds. Thus 3D SENSE DE technique uses a fraction of the time and needs far less patient co-operation than the conventional 2D DE technique, while providing equivalent image quality when performing cardiac imaging for irreversible myocardial injury.

300. 3D Magnetization-Prepared TrueFISP: Initial Clinical Evaluation of a New MR Technique for Imaging Coronary Arteries

Richard Mc Carthy,[1] James Carr,[1] Vibhas Deshpande,[1] Steven Shea,[1] Jordin Green,[1] J. Paul Finn,[1] Debiao Li.[1]
[1]*Department of Radiology, Northwestern University Medical School, 448 East Ontario Street, Chicago, Illinois, USA*

Introduction: TrueFISP (Fast Imaging with Steady-state Precession) is a MR imaging technique which has recently gained wide acceptance in cardiovascular imaging. It produces images with high signal-to-noise ratio (SNR) and high blood/myocardium contrast-to-noise ratio (CNR).

As human coronary arteries are surrounded by a lipid environment, fat suppression is essential for effective coronary artery imaging. The combination of ECG-triggered,magnetization-prepared, segmented 3D TrueFISP imaging and a breath-hold volume targeted approach has recently been described for coronary MRA. In this method fat suppression is achieved by employing a magnetization preparation scheme and a fat saturation pulse. This technique has been shown to produce fat suppressed coronary MRA images with high SNR and CNR in healthy volunteers.

Purpose: We have instituted a study to evaluate the effectiveness of this new tecnique in patients with coronary artery disease.

Methods: Patients who had recently undergone (within the preceding two months) or were about to undergo conventional coronary angiography at our institution were approached to have a coronary MR angiogram as part of this research project. Patients who had any contraindications to MR were excluded from the study. Additionally any patients who had undergone an angioplasty with or without coronary stent insertion were excluded. Informed consent was obtained for each patient. The MRI examinations were performed on a 1.5 T whole body scanner [Siemens Magnetom Sonata, Erlangen, Germany] with a high performance gradient sub-system (maximum gradient strength: 40 mT/m, maximum slew rate: 200 mT/m/msec). A

Figure 1. Conventional angiogram showing a significant stenosis of the LAD (arrow).

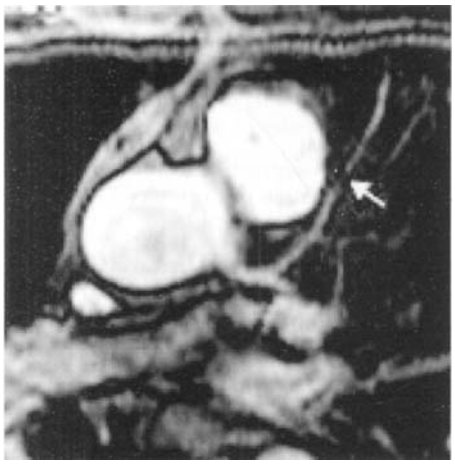

Figure 2. TrueFISP coronary MRA in the same patient as Figure 1, showing a significant stenosis of the LAD, corresponding to that seen on conventional angiography.

3D segmented echo-planar scout scan was first acquired to cover a major portion of the heart. Orientations of the left main (LM) and left anterior descending (LAD) coronary arteries and the right coronary artery (RCA) were determined using multiplanar reconstructions from the volume localizer scan. Two breath-hold, 3D segmented True-FISP scans were then performed to target the left and right coronary arteries respectively. Imaging papameters included: TR/TE = 3.8/1.9 msec; flip angle = 50°; number of lines per cardiac cycle = 25–31; FOV = (175–195) × (260–280) mm^2; matrix size = (75–100) × 256; slab thickness = 24–32 mm; number of partitions = 8 (interpolated to 16); and the scan time = 24–30 heartbeats. A magnetization-preparation scheme with a spectral fat saturation pulse followed by an $\alpha/2$ preparation (α = flip angle for data acquisition) and 20 dummy cycles was employed to achieve fat saturation and reduced image artifacts.

The images were evaluated by an observer experienced in coronary MRA. Each vessel was assessed as having or not having a hemodynamically significant stenosis [>50%]. The results were compared to those of conventional catheter coronary angiography.

Results: A total of 17 patients have been studied with the described protocol. MR images from two patients were discarded from further analysis because of the inadequate image quality resulting from poor ECG signals. In the remaining 15 patients, good image quality was obtained. Each patient did not have all of the major coronary vessels assessed by MRA. A total of 35 vessels were assessed in 15 patients. The accuracy for detection of hemodynamically significant coronary artery stenoses was 83%, the sensitivity was 70% with a specificity of 88%.

Conclusion: Our intial clinical experience with this new technique is encouraging. Thus far, the number of patients is small and the study is currently in progress, but we feel confident that with greater numbers of patients and greater experience on our part that the figures for sensitivity and

specificity will improve. We feel that this technique is promising for coronary MRA. Further improvements in spatial resolution will enhance the diagnostic value of the technique.

301. The Effect of Contrast Dose and Quantitation Method on the Estimation of Coronary Flow Reserve by 1st-Pass MRI Myocardial Perfusion

Timothy Christian,[1] Anthony Aletras,[2] Robert Balaban,[1] Andrew Arai.[1] [1]*National Institutes of Health, NHLBI, LCE, Bethesda, Maryland United States;* [2]*National Institutes of Health, Building 10/Room B1D-416, Bethesda, MD United States*

Introduction: Myocardial perfusion imaging is frequently combined with vasodilator stress to detect regional abnormalities in coronary flow reserve (CFR). Analysis is often visual or semiquantitative and dependent on adequate signal intensity (SI) to noise. Consequently, there should be advantages for using higher contrast doses.

Purpose: To compare the impact of Gd-DTPA concentration ([Gd]) on semiquantitative measures of myocardial blood flow (MBF) during vasodilator stress for 1st-pass myocardial multislice perfusion imaging. These measures by [Gd] will be compared with absolute measures of MBF using deconvolution techniques.

Methods: Six beagles were instrumented to permit local adenosine (20 μgm/min/kg) infusion in a coronary artery. Gd-DTPA was infused in 6 dogs at three doses per dog: 0.025, 0.05 and 0.10 mmol/Kg while running a saturation recovery EPI perfusion sequence with a temporal resolution of 137 msec. Microspheres were injected directly after each infusion for MBF determination. The contrast enhancement ratio (CER) was derived as follows: (peak SI − baseline SI)/baseline SI. Absolute MBF was calculated as follows: a serial double bolus method was used to provide both an arterial input function within the range of linearity of SI to [Gd] followed by a high [Gd] bolus for maximal myocardial enhancement. The low [Gd-DTPA] bolus was 0.0025 mmole/Kg and the high [Gd-DTPA] bolus was 0.10 mmole/Kg. Absolute quantitation was performed using Fermi function deconvolution techniques.

Results: MBF in adenosine zones and control zones did not differ significantly by [Gd] (see table below). Mean CER increased linearly with higher [Gd] in both adenosine and control zones. However, the CER exhibited a plateau effect during adenosine infusion at all [Gd] with higher MBF values. When fully quantitative Fermi function analysis was used, the relationship between MBF and MRI measures remained linear through all MBF ranges.

Conclusion: CER increased in a linear manner with increasing [Gd] but demonstrated a plateau response when analyzed with absolute MBF by microspheres at the higher flow ranges seen with adenosine hyperemia. No such plateau effect was seen when this same data was analyzed with Fermi function deconvolution quantitative techniques. The quantitative double bolus method described here combines the advantages of linearity with MBF through all ranges with enhanced SNR of higher [Gd]. For vasodilator stress, fully quantitative methods appear necessary to accurately determine regional CFR.

302. Comparison of Stress Perfusion Magnetic Resonance Imaging with Sestamibi SPECT in Established Coronary Artery Disease

Richard Coulden,[1] Timothy Gray,[1] Emer Sonnex,[1] Martin Graves,[2] Peter Schofield.[1] [1]*Papworth Hospital, Papworth Everard, Cambridge, England, United Kingdom;* [2]*Addenbrooke's Hospital, Hills Rd, Cambridge, England, United Kingdom*

Introduction: Ultrafast MR imaging (MRI) during intravenous contrast enhancement offers new possibilities for the assessment of myocardial perfusion. The technique can be performed quickly and safely with adenosine stress and has several advantages over other non-invasive tests for ischemia [1,2]. Correlation with coronary angiography, however, has shown only moderate sensitivity and specificity. Coronary angiography, although the accepted 'gold standard' for assessing coronary artery disease, may not be the best comparator for a perfusion test. Angiography defines vessel anatomy but cannot quantify flow or allow accurate assessment of the contribution of collateral flow.

Purpose: To compare a multislice first pass myocardial perfusion technique before and after adenosine stress with radionuclide scintigraphy before and after adenosine stress.

Methods: 23 patients with coronary artery disease diagnosed by angiography (> than 70% stenosis in any major vessel) were enrolled. All examinations were performed on a 1.5T magnet system (GE Signa CV/i). The pulse sequence used consists of a notched preparation followed immediately by an interleaved gradient-echo echo-planar sequence [3]. Depending on heart rate, 5–7 short axis slices were obtained on alternate beats for 80 beats during a breath-hold. For the stress study, a bolus injection of GdDTPA (0.1 mmol/kg at 5 mls/sec plus saline chaser) was given intravenously from the antecubital fossa at

Table 1

MBF Values

	[Gd] 0.025	[Gd] 0.05	[Gd] 0.10	p of [Gd]
Adenosine	2.84 ± 1.2	1.80 ± 1.2	2.58 ± 1.4	NS
Control	0.57 ± 0.19	0.63 ± 0.23	0.67 ± 0.15	NS
p of zone	<0.002	<0.05	<0.05	

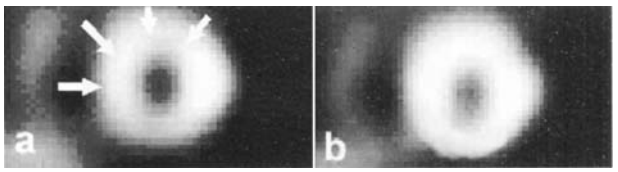

Figure 1. (a) stress and (b) rest short axis 99m Tc sestamibi images showing reversible anterior and septal perfusion defect (arrows).

3 minutes of a 4 minute adenosine infusion (140 mcg/kg/min). This was repeated at rest 20 minutes later. Radionuclide SPECT was performed within 4 weeks of the MRI using 400 MBq 99m Tc sestamibi on each day of a standard 2 day protocol (Elscint Apex4). For the stress study, sestamibi was injected after 3 minutes of a 6 minute adenosine infusion (140 mcg/kg/min) with imaging at 1 hr. Rest imaging was performed the following day. Images were assessed independently by blinded observers using a 16 segment model. Segments were defined as normal or abnormal (>50% of the segment showing ischemia). Because of problems with slice and rotational mismatch, MRI and sestamibi images re-reported by direct comparison both observers together.

Results: Using radionuclide scintigraphy as the 'gold standard' with 2 observers scoring MR and scintigraphy independently, MR perfusion imaging during stress had a sensitivity of 42% and specificity of 86% for identifying reversible ischemia (368 analysable segments). The poor sensitivity appeared to be due to problems registering the 4 short axis scintigraphic reconstructions with the 5–7 MR slices. After slice matching the 2 observers re-read both studies together. This improved sensitivity and specificity to 73% and 87% respectively.

Conclusion: On blinded reading, MR perfusion imaging correlates poorly with scintigraphy. This improves significantly when MR and scintigraphic images are matched highlighting the difficulty of comparing two very different techniques. Observed scintigraphic 'perfusion' is a product of myocardial perfusion, wall motion and muscle mass while MR perfusion potentially reflects only perfusion. One must add to this the problems of accurate segmental registration while maintaining a blinded read. This study confirms the potential of this sequence for assessing myocardial perfusion but a more robust comparison with existing technques is essential. Design of future studies will be crucial. In particular, great care will be needed to eliminate errors due to mis-registration or marked wall motion abnormality. This would be best acheived by comparison of gated SPECT and MR perfusion and using parametric maps to report both. For MR, however, new analysis tools will be needed before this can be done.

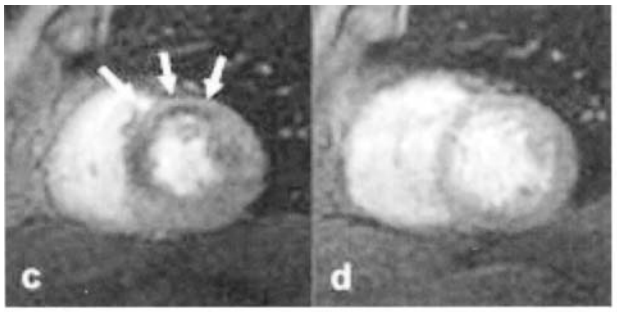

Figure 2. (c) stress (d) rest MR perfusion images at the same level showing matching reversible defect (arrows).

303. Color-Encoded Semiautomatic Analysis for Multi-Slice First-Pass Magnetic Resonance Perfusion: Comparison to 99m Technetium Single-Photon-Emission-Computed-Tomography

Holger Thiele,[1] Sven Plein,[2] Marcel Breeuwer,[3] John Ridgway,[2] Dave Higgins,[2] Penelope Thorley,[2] Gerhard Schuler,[1] Mohan Sivananthan.[2] [1]*University of Leipzig, Department of Cardiology, Leipzig, Sachsen, Germany;* [2]*Leeds General Infirmary, Gt. George Street, Leeds, West Yorkshire, United Kingdom;* [3]*Philips Medical Systems - Building QV 162, P.O. Box 10.000, Best, Netherlands Netherlands*

Introduction: First pass myocardial perfusion MR imaging has been shown to reliably detect coronary artery disease. It is commonly accepted practice to analyze the upslopes of the myocardial signal during the 1st pass and to calculate the myocardial perfusion reserve index (MPRI) by dividing the stress upslope by the rest upslope after correction for the left ventricular input function. However, the absence of efficient, easy and reliable image analysis software is an obstacle for the Introduction: of this method into clinical practice.

Purpose: In this study we tested whether a new prototype software, which generates the MPRI semiautomatically and displays it in color-encoded maps, can be used for detection of perfusion defects.

Methods: Twenty-four patients underwent both 99m Technetium single-photon-emission-computed-tomography (SPECT) and first-pass magnetic resonance perfusion imaging under rest and stress using adenosine at standard dose (140microg/kg/min). SPECT images were acquired with a gamma camera (Park Isocam II). Thirty-two planar images were obtained (64 × 64 pixel matrix, 15 sec per image, 40 cm

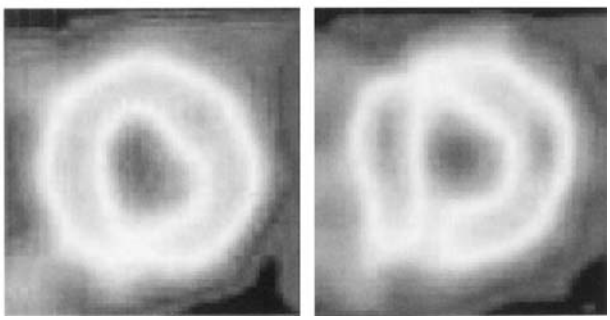

Figure 1. SPECT Rest versus Stress.

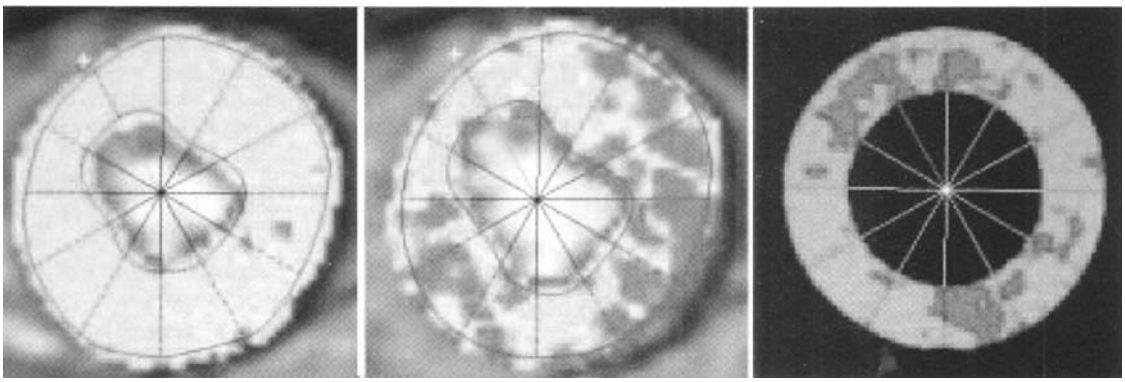

Figure 2. MR Rest versus Stress and MPRI.

Table 1

	SPECT+	SPECT −	
MR+	39	20	59
MR −	9	124	133
	48	144	192

FOV, voxel size 6.25 × 6.25 × 6.25 mm). MR images were acquired on a 1.5 Tesla MR system (Intera CV, Philips, The Netherlands). Four short axis slices of the heart were acquired every heart beat using an ECG-gated T1-weighted inversion recovery turbo gradient echo sequence with sensitivity encoding (TR 3.1 ms, TE 1.6 ms, flip angle 15°, FOV 350-450 mm, matrix 160 × 112, reconstructed to 256 256, SENSE-factor 2). At end-expiratory breath hold a bolus of 0.05 mmol/kg bodyweight gadolinium-DTPA (Magnevist, Schering AG, Berlin, Germany) was rapidly injected into a peripheral vein under rest and stress conditions.

Off-line image analysis was performed on a dedicated workstation using prototype software (EasyScil, Medical Imaging Information Technologies—Advanced Development, Philips Medical Systems, The Netherlands). The endocardial and epicardial borders were drawn manually. The maximal upslopes of the myocardium and the left ventricle were calculated automatically from the average time-intensity profiles and displayed as color overlays on the original images. The perfusion parameters derived from rest and stress studies were then compared on a pixel-to-pixel basis to calculate the MPRI with automated correction for the left ventricular input function. Perfusion defects were defined visually, if there was a region of a lower MPRI in contrast to normal segments of the same patient. All SPECT studies were analyzed in the conventional manner using a subjective scale in each segment in comparison to the maximal pixels of the heart. The entire SPECT study was analyzed, however, for comparison with MR only the results for short axis slices were used.

Results: All images obtained were of adequate quality for image analysis. All patients had at least one inducible or fixed defect. Positive and negative results for segments for both imaging techniques are shown in the table. Taking SPECT as a reference method, it resulted in a sensitivity of 81%, specificity of 86%, positive predictive value of 66% and negative predictive value of 93% for MR. Especially in inferior slices, where attenuation can impair SPECT images, many discrepant results were found.

Conclusion: Post-processing of first pass myocardial perfusion MR imaging using a new semiautomatic software, which easily generates the MPRI and displays it visually as color-encoded images has a high sensitivity and specificity for detection of perfusion defects in comparison to SPECT. This post-processing method may accelerate the time-consuming analysis of MR perfusion images thus enabling a more widespread clinical utility.